Evidence for Photocatalyst Involvement in Oxidative Additions of Nickel-Catalyzed Carboxylate *O*-Arylations

Jamal A. Malik,[†] Amiera Madani,[†‡] Bartholomäus Pieber,*[†] and Peter H. Seeberger*[†‡]

[†]Department of Biomolecular Systems, Max-Planck-Institute of Colloids and Interfaces, Am Mühlenberg 1, 14476 Potsdam, Germany.

‡Department of Chemistry and Biochemistry, Freie Universität Berlin, Arnimallee 22, 14195 Berlin, Germany.

SUPPORTING INFORMATION

TABLE OF CONTENTS

1. General remarks

Substrates, reagents, and solvents were purchased from commercial suppliers and used without further purification unless otherwise noted. *N*-Boc proline was lyophilized for 24h prior to use to remove residual water. *N-tert*-butylisopropylamine (BIPA) was prepared according to literature procedure.[1] ^{1}H- and ^{13}C-NMR spectra were obtained using a Varian 400 spectrometer (400 MHz, Agilent), an Ascend^{TM} 400 spectrometer (400 MHz, cryoprobe, Bruker) and a Varian 600 spectrometer (600 MHz, Agilent) at 298 K, and are reported in ppm relative to the residual solvent peaks. Standard NMR quantification was through Varian 400 MHz spectrometer, with the following settings: Acquisition points (complex points) 16384; Acquisition time 2.556s; Relaxation delay 1.000s; Receiver gain as autogain (default 30); Spectral width 16.0 ppm; 128 scans. Peaks are reported as: s = singlet, d = doublet, t = triplet, q = quartet, m = multiplet or unresolved, with coupling constants in Hz. No thin-layer or otherwise silica-based chromatography was performed in the course of these experiments. Lamps (A160, 40W maximum) were purchased from Kessil and used as received. *In situ* FTIR analysis was performed with a ReactIR^{TM} 15 (Mettler-Toledo) console, with a DST 9.5mm SiComp^{TM} probe attached. Data processing from *in situ* FTIR analysis was performed in Microsoft Excel. Graphs were presented in Microsoft Excel or Origin.

2. General procedures and analysis for *in situ* ReactIR experiments

2.1.1 Considerations before experiments

Roughly two hours prior to each experiment, the ReactIR console was purged and filled with liquid nitrogen. A background spectrum was recorded shortly before attaching the reaction vessel to the ReactIR probe. To maintain a constant operating temperature during the course of longer experiments, the ReactIR console was replenished with new liquid nitrogen every 12 hours.
The 440 nm lamp was permanently affixed to a metal rod such that the edge of the lamp was 3.5 cm from the middle of the diameter of the ReactIR probe. During our initial studies we found that the greatest source of error derived from inconsistencies in lamp distance and orientation. As such, neither the 440 nm lamp nor ReactIR probe were moved nor disturbed during the months required for data collection.

2.1.2 General experimental procedure

A custom-made vial with a sidearm attached (19 x 100 mm, see Figure S1) was equipped with a stir bar and charged with photocatalyst, *N*-Boc proline, and aryl iodide. Subsequently, DMSO (anhydrous, 3 mL), $NiCl_2$·glyme and dtbbpy from a stock solution, and BIPA were added. Both necks of the vial were sealed with septa and Parafilm. The reaction mixture was sonicated for 5 min followed by stirring for 5-10 min until fine dispersion of the solids was achieved. The flask was then transported to the ReactIR where the larger septum was removed and the vessel immediately attached to the probe. To ensure an airtight seal, a PTFE adapter was affixed to the probe, to which the vessel was snugly attached. The vessel was continually degassed with Ar for 15 minutes through the sidearm with thin needles. The mixture was stirred for 5 minutes again to re-ensure mixing of the components while data collection started on the ReactIR. After this period the 440 nm lamp was turned on, and this initiation time was marked with the ReactIR proprietary software.

2.1.3 General experimental procedure for delayed injection experiments

A custom-made vial with a sidearm attached (19 x 100 mm, see Figure S1) was equipped with a stir bar and charged with all reaction components except for one. Both necks of the vial were sealed with septa and Parafilm. The reaction mixture was sonicated for 5 min followed by stirring for 5-10 min until fine dispersion of the solids was achieved. The flask was then transported to the ReactIR, where the larger septum was removed and the vessel immediately attached to the probe. To ensure an airtight seal, a PTFE adapter was affixed to the probe, to which the vessel was snugly attached. The vessel was continually degassed with Ar for 15 minutes through the sidearm with thin needles. The mixture was stirred for 5 minutes again to re-ensure mixing of the components while data collection started on the ReactIR. After this period the 440 nm lamp was turned on to 100% power, and this initiation time was marked with the ReactIR proprietary software. After five minutes, the last component (in a DMSO solution) was injected.

2.1.4 Considerations after experiments

To aid in separation of peaks, a negative second derivative function was applied to the raw ReactIR absorbance data. After subtraction of reference spectra, the product peak arrives at ~1764 cm^{-1} while disappearance of the starting material can be observed at a peak around ~761 cm^{-1}. Raw data from iCiR was ported to Excel (Microsoft) for processing. Final data were then plotted in Excel (Microsoft) or OriginPro 2015 (OriginLab).

Initial concentrations of all starting materials were determined from reaction stoichiometry. Final concentration of the product was determined from ^{1}H-NMR analysis. This method was validated as described in Section 3.

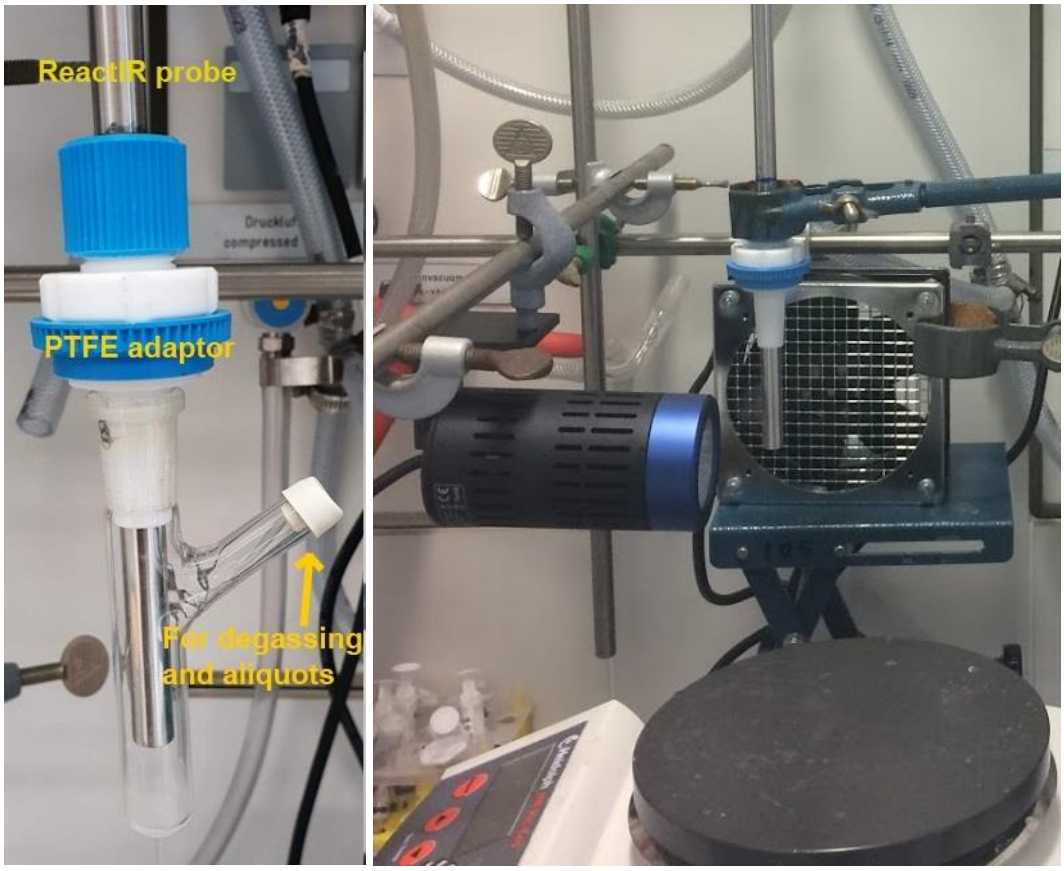

Figure S1. (A) Vessel used for kinetics experiments with sidearm attached to enable degassing after attachment to the ReactIR probe. (B) Setup shown without attached vessel. As our largest source of error was found to derive from inconsistency in lamp placement, a secured lamp and probe were left unchanged for all experiments in this study.

2.2 NMR analysis of reactants, products, and side products

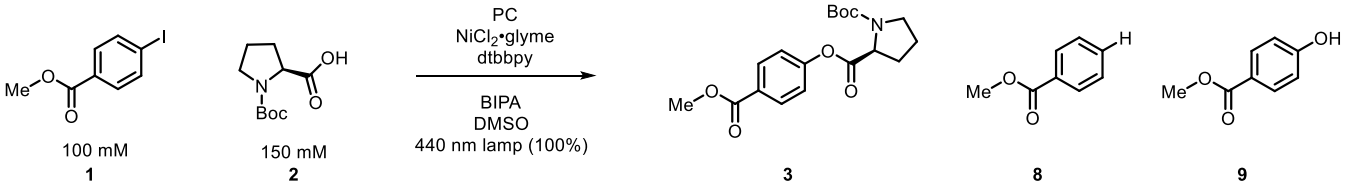

Sample NMRs are shown below.

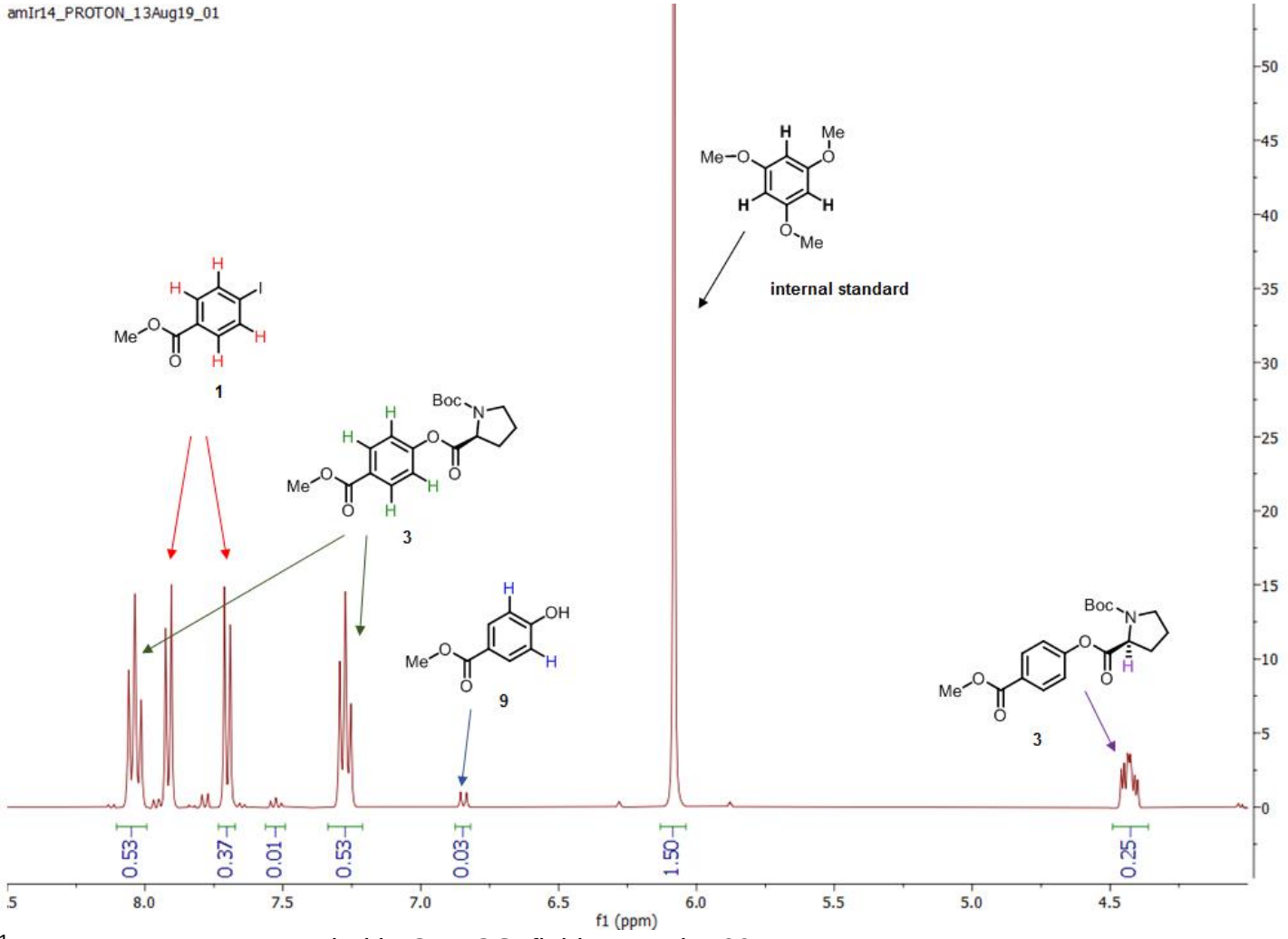

^{1}H proton spectrum recorded in C_2D_6OS, field strength 400 MHz.

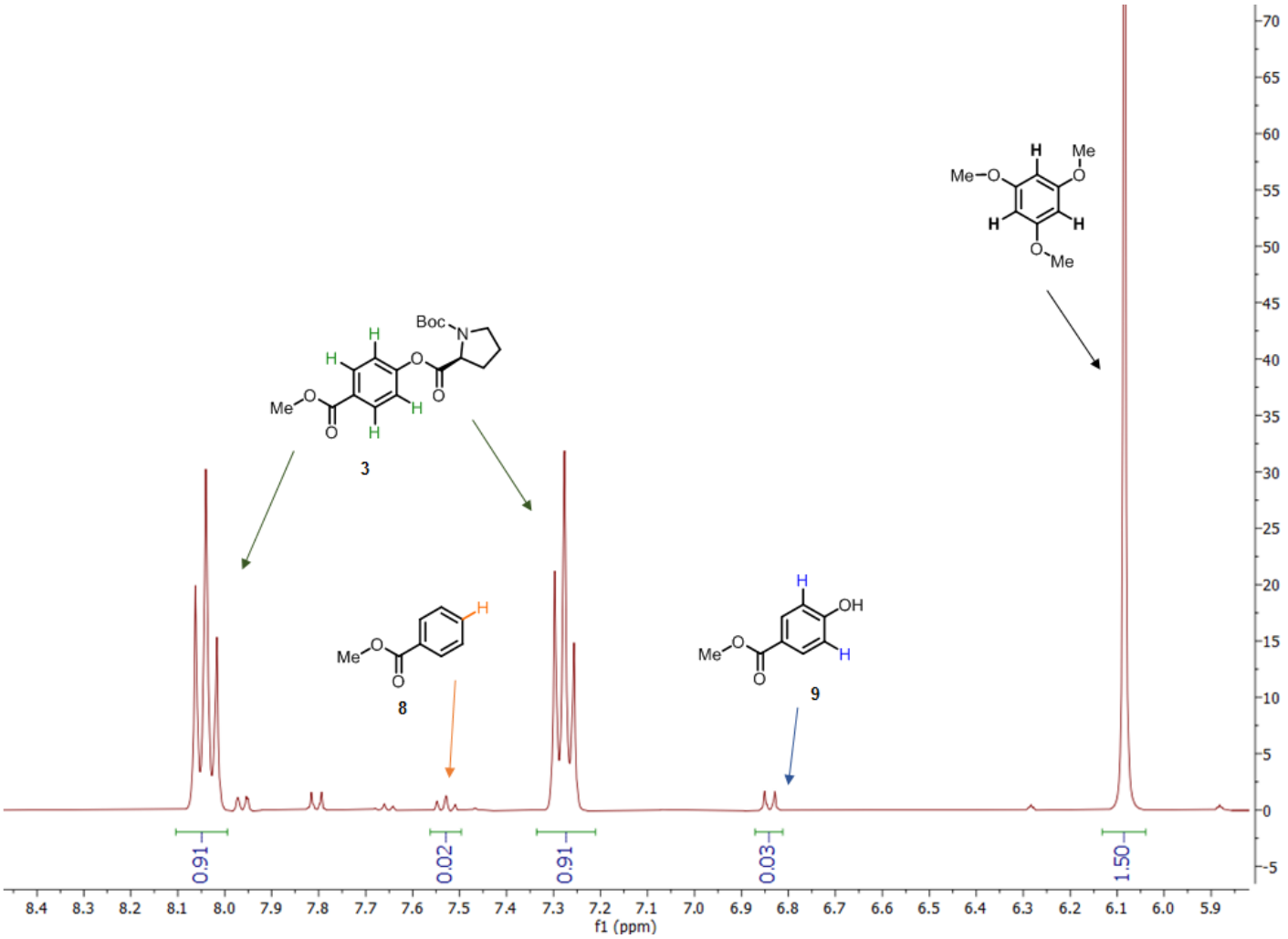

^{1}H proton spectrum recorded in C_2D_6OS, field strength 400 MHz.

Sample completed, selective reaction.

3. On the validity and reproducibility of data

3.1 Ensuring validity of data

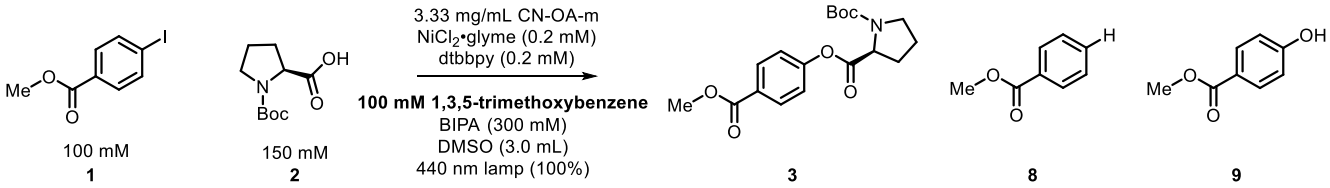

Scheme S1. Experiment to independently validate the method.

An experiment following the general procedure outlined (see 2.1.2) above was conducted, according to the stoichiometry in Scheme 1. Notably, added to the normal reaction mixture was 100 mM 1,3,5-trimethoxybenzene, the internal standard used for all *ex situ* NMRs.

Upon initiation of light and periodically thereafter, small aliquots were withdrawn. The timepoints of these aliquots were noted, and each aliquot was analyzed with ^{1}H-NMR.

Previously we have demonstrated that final NMR yield of these reactions is accurately reflected by isolated yield.[2] As such, NMR can be considered a reliable benchmark for comparison of our *in situ* method.

ReactIR yield was calculated from raw absorbance data that was normalized and scaled, tethered to the final NMR yield. The overlay below between two completely independent methods indicates that ReactIR is a competent measure of reaction progress.

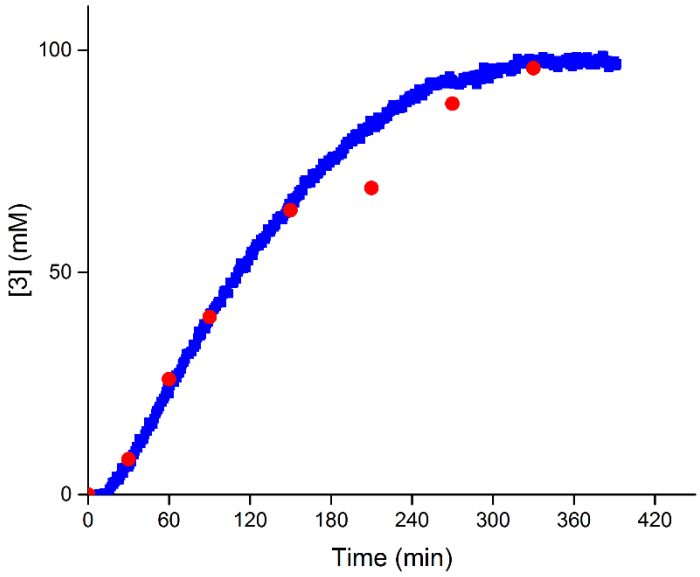

Figure S2. Correlation of NMR and IR yield.

Time (min)	NMR Yield	IR Yield	Difference	NMR SM	Total mass balance
0	0	0	0	98	98
30	8	6.2	1.8	87	95
60	26	22.7	3.3	72	98
90	40	40.7	-0.7	57	97
150	64	64.4	-0.4	33	97
210	69	83	-14	18	87
270	88	93.2	-5.2	6	94
330	96	97.7	-1.7	2	98

Table S1. NMR was used to validate *in situ* infrared tracking as a valid experimental technique to determine reaction progress.

3.2 Ensuring reproducibility of data

Frequently experiments were repeated to ensure that data was reproducible. Below are shown one example of such a data set.

In general, for data sets that were to be compared with one another, the same stock solution of $NiCl_2$•glyme and dtbbpy was used. As stated above, the lamp was secured and unmoved during the course of all experiments for this work. Those two factors were paramount for reproducible data collection.

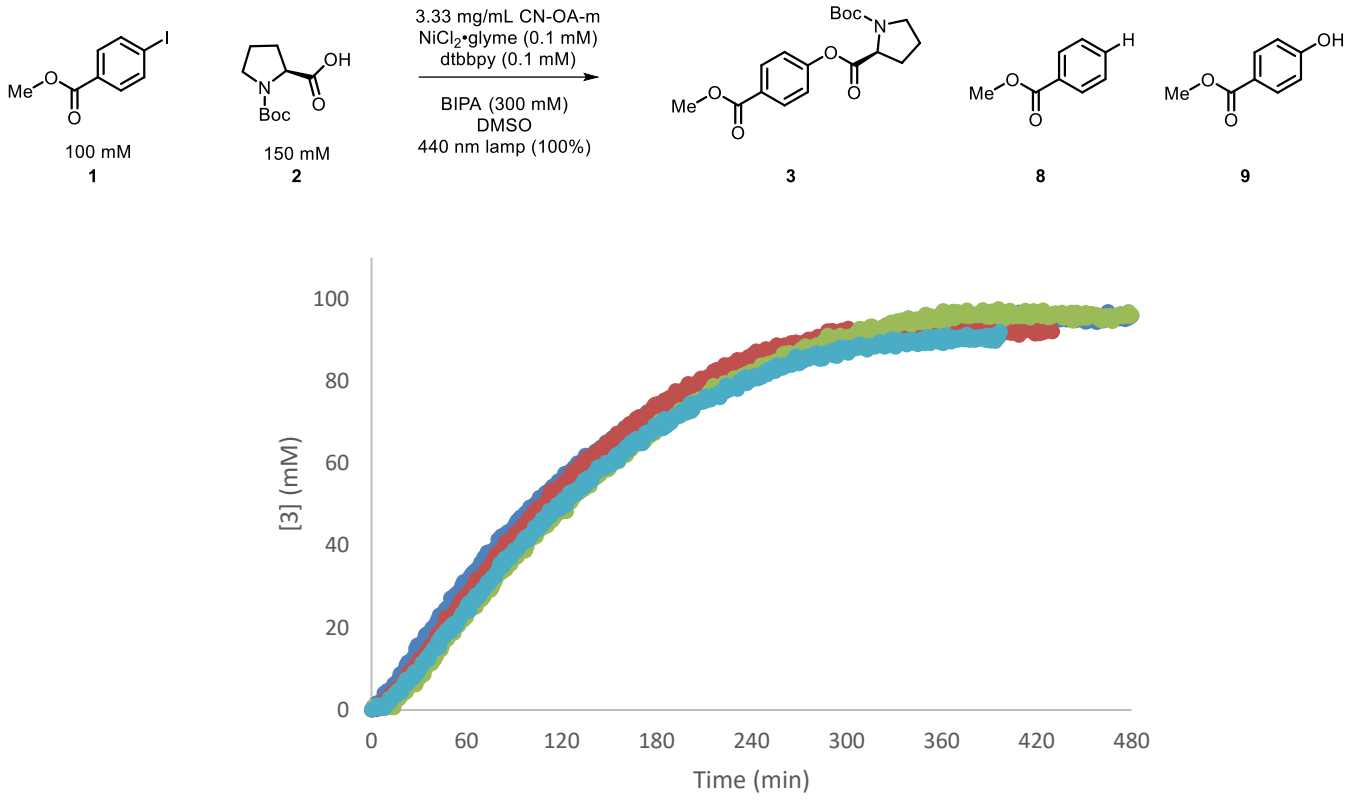

Figure S3. Photon-unlimited, heterogeneous reactions run in quadruplicate to verify reproducibility.

Entry	[1]	[3]	[8]	[9]	Total
jam260	0	91	4	4	99
jam264	0	92	4	4	100
jam266	0	91	4	5	100
jam267	3	89	3	2	97

Table S2. Tabulated yields and side products from quadruplicate quality control testing.

Two of these NMRs are shown below.

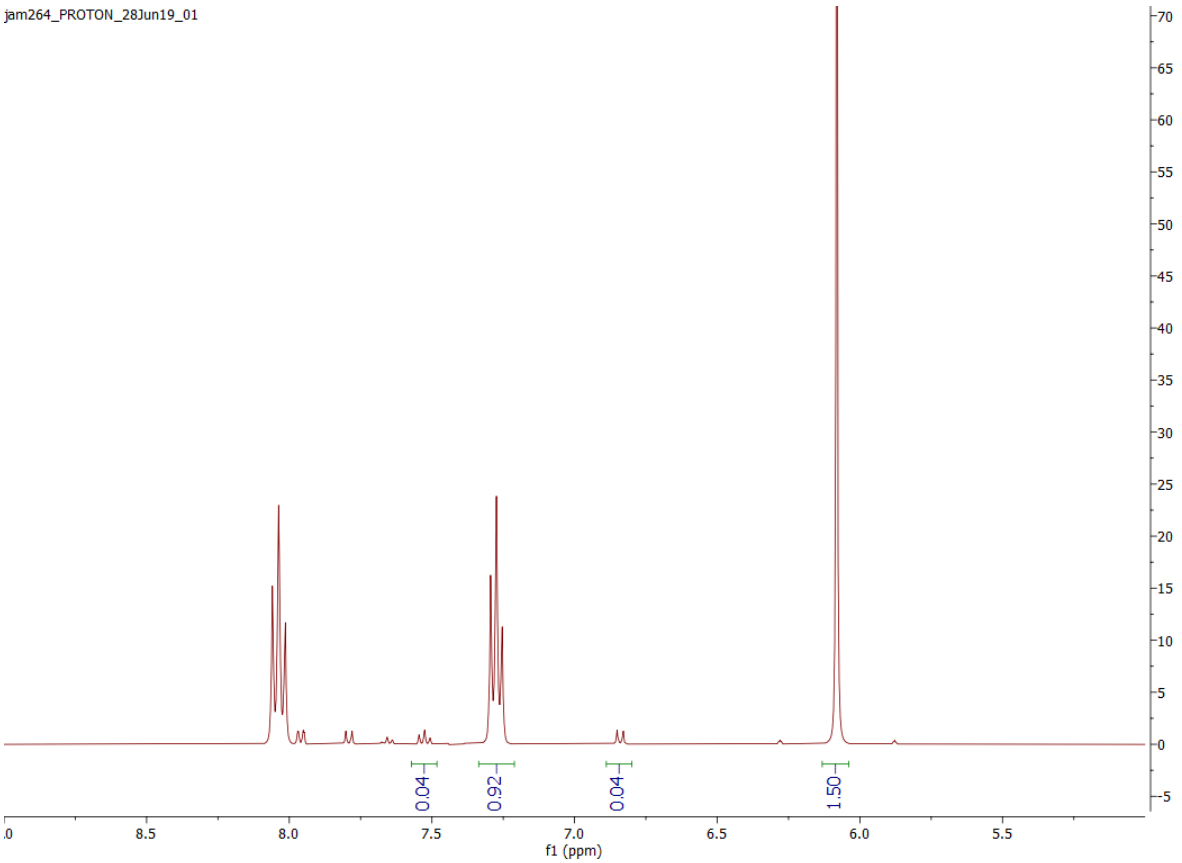

^{1}H proton spectrum recorded in C_2D_6OS, field strength 400 MHz. (92% **3**, 4% **8**, 4% **9**)

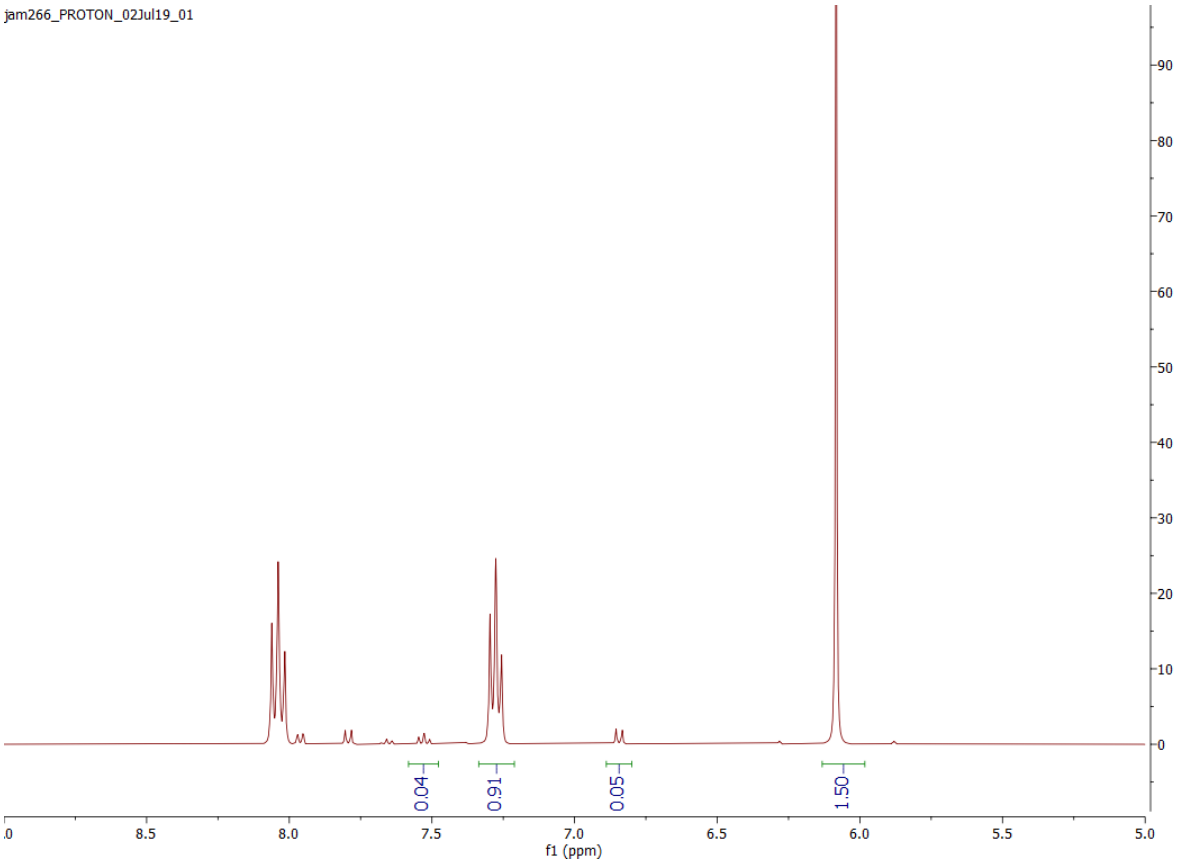

^{1}H proton spectrum recorded in C_2D_6OS, field strength 400 MHz. (91% **3**, 4% **8**, 5% **9**)

4. Graphitic carbon nitride (heterogeneous) as photocatalyst: Photon-limited regime

4.1 Effect of lamp power

Following the general procedure outlined above, the four different settings on the 440 nm lamp were tested.

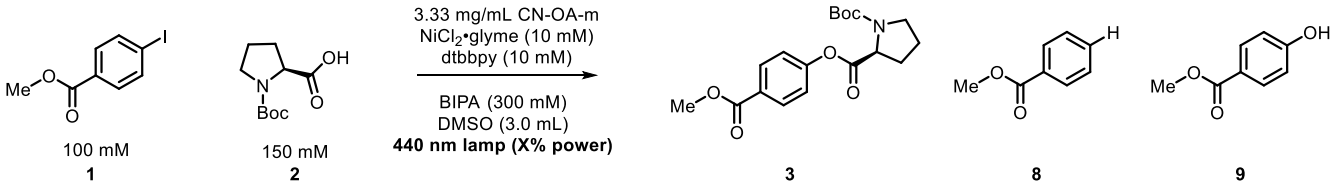

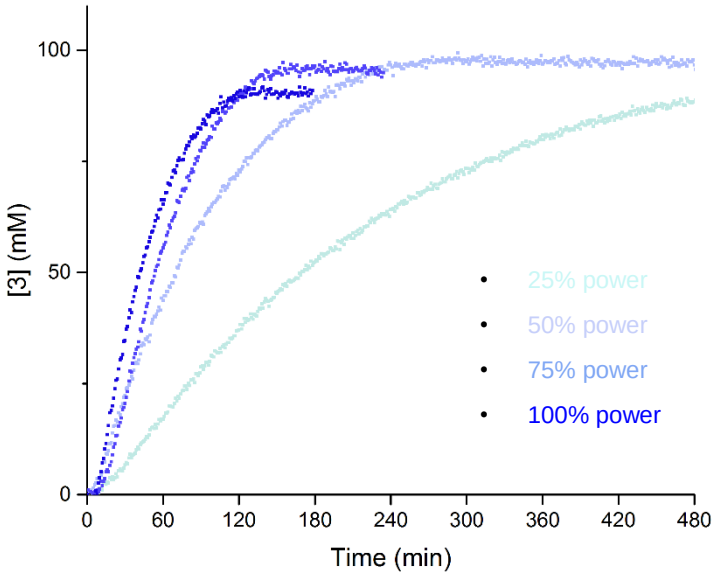

Figure S4. Effect of lamp power on reaction speed. In order to best saturate the nickel catalyst with excited photocatalytic species, the highest lamp setting was chosen for "photon-unlimited" experiments in this study. 50% power was used for the "photon-limited" studies due to slightly advantageous yield.

Entry	Lamp	[1]	[3]	[8]	[9]	Total
jam176	**25**	0	89	3	3	95
jam178	**50**	0	94	2	3	99
jam179	**75**	0	89	3	2	94
jam180	**100**	0	90	3	2	95

Table S3. Tabulated yields and side products from screening lamp power.

4.2 Cursory examination of induction period

A custom-made vial with a sidearm attached (19 x 100 mm, see Figure S1) was equipped with a stir bar and charged with all reaction components except for one. Both necks of the vial were sealed with septa and Parafilm. The reaction mixture was sonicated for 5 min followed by stirring for 5-10 min until fine dispersion of the solid photocatalyst was achieved. The flask was then transported to the ReactIR, where the larger septum was removed and the vessel immediately attached to the probe. To ensure an airtight seal, a PTFE adapter was affixed to the probe, to which the vessel was snugly attached. The vessel was continually degassed with Ar for 15 minutes through the sidearm with thin needles. The mixture was stirred for 5 minutes again to re-ensure mixing of the components while data collection started on the ReactIR. After this period the 440 nm lamp was turned on to 100% power, and this initiation time was marked with the ReactIR proprietary software. After five minutes, the last component (in a DMSO solution) was injected.

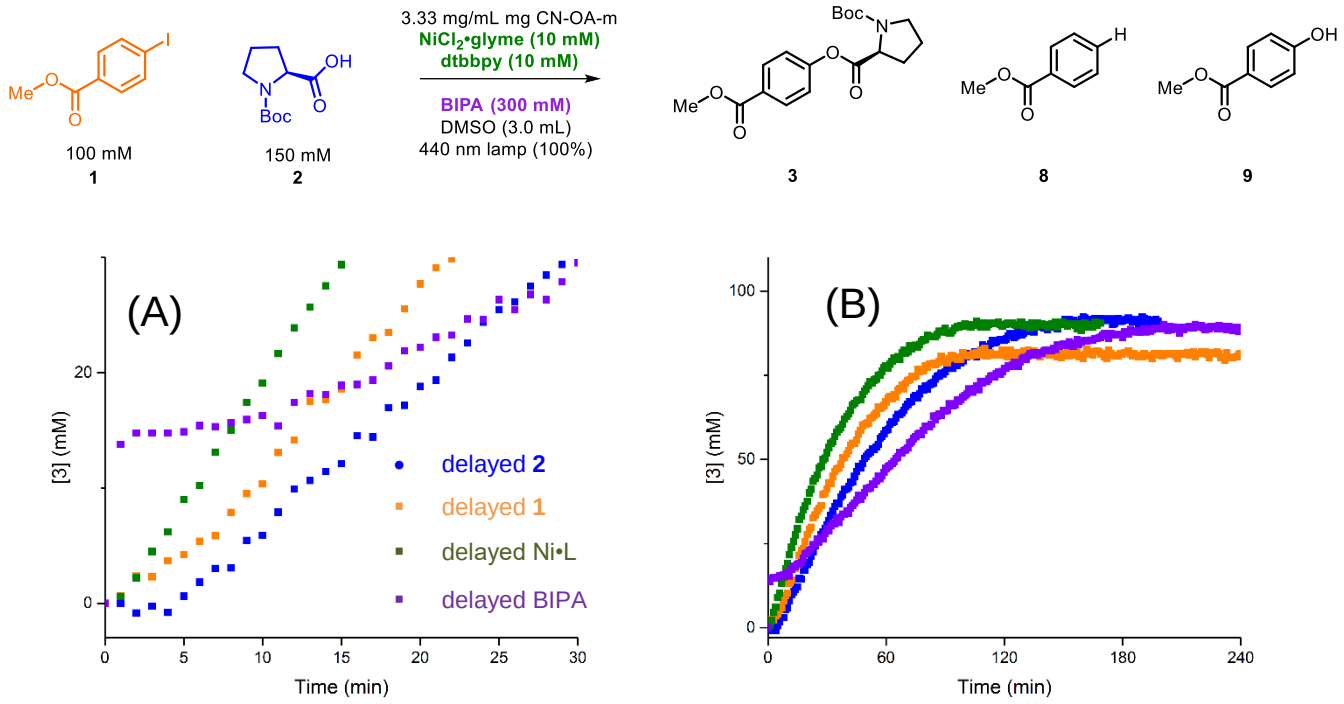

Figure S5. Delayed injection experiments in order to obtain rough information about what contributes to the induction period. Immediate, positive-order kinetics are observed upon delayed injection of the nickel and of the aryl iodide. Delayed injection of proline retains the induction period. Delayed injection of the base results in catalyst activation-type behavior. (A) First 30m, zoomed. (B) Complete reaction.

Entry	Delayed reagent	[1]	[3]	[8]	[9]	Total
jam183	aryl iodide (**1**)	0	80	4	3	87
jam182	N-Boc proline (**2**)	0	91	3	1	95
jam184	Ni • L	0	90	3	2	95
jam185b	Base (BIPA)	0	91	3	1	95

Table S4. Tabulated yields and side products from delaying injections of reagents.

4.3 Order of catalyst, photon-limited

Following the delayed injection procedure (see section 2.1.3 – Ni•L delayed) described above, experiments were conducted varying only the concentration of nickel and ligand.

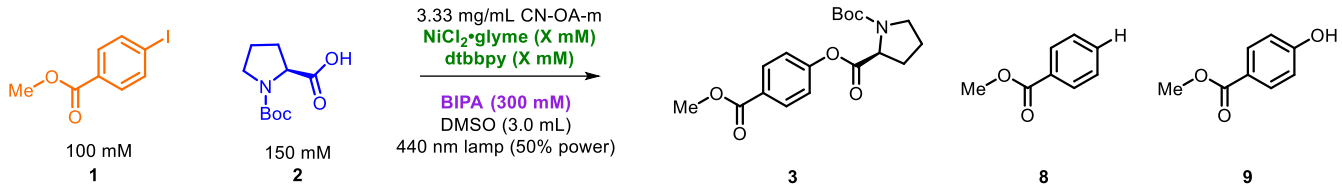

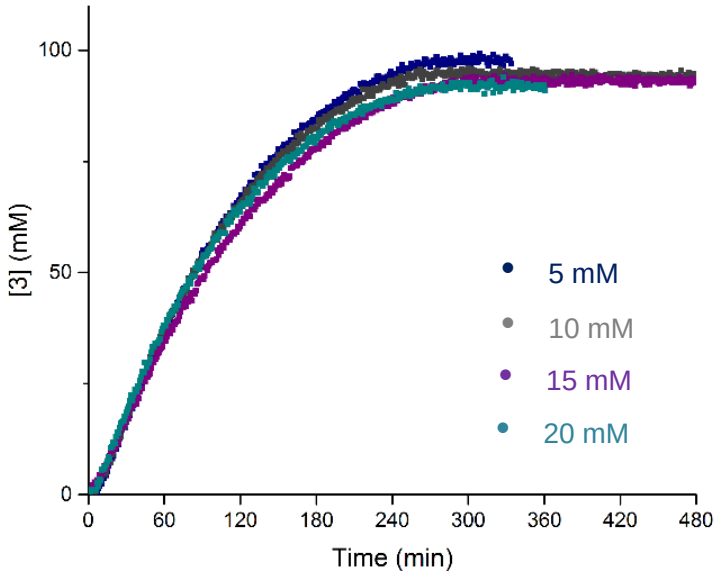

Figure S6. In the photon-limited regime, catalyst concentration has no effect on product-forming rate, and is therefore zero-order. Delayed injection of $NiCl_2$•glyme and dtbbpy solution was used to assist potential VTNA manipulations, which were not used in this instance.

Entry	[Ni•L]	[1]	[3]	[8]	[9]	Total
jam209	5	0	96	3	2	101
jam208b	10	0	92	3	3	98
jam210	15	0	94	2	2	98
jam211	20	0	91	3	2	96

Table S5. Tabulated yields and side products from varying catalyst order in photon-limited regime.

4.4 Effect of photocatalyst

Following the delayed injection procedure (see section 2.1.3 – Ni•L delayed), two experiments were conducted varying only the amount of photocatalyst.

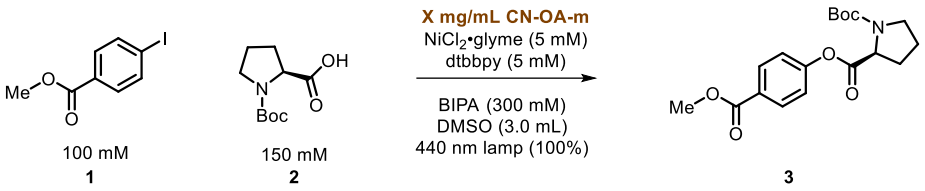

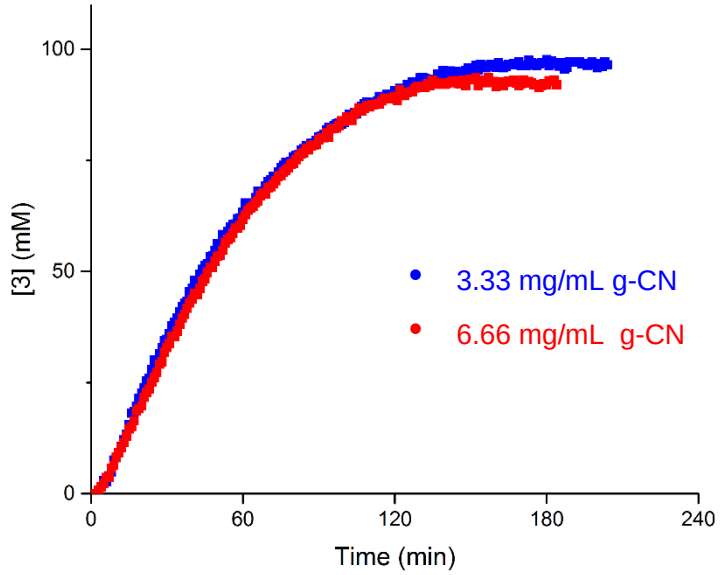

Figure S7. In the photon-limited regime, doubling the amount of photocatalyst has no effect on reaction rate. Delayed injection of $NiCl_2$•glyme and dtbbpy solution was used to assist potential VTNA manipulations, which were not used in this instance.

Entry	PC loading	[1]	[3]	[8]	[9]	Total
jam220	3.33 mg/mL	0	95	2	1	98
jam221	6.66 mg/mL	0	91	4	3	98

Table S6. Tabulated yields and side products from varying photocatalyst loading.

4.5 Same excess

Following the delayed injection procedure (see section 2.1.3 – Ni•L delayed), two experiments were conducted with the same "excess" (50 mM) between $[1]_0$ and $[2]_0$.

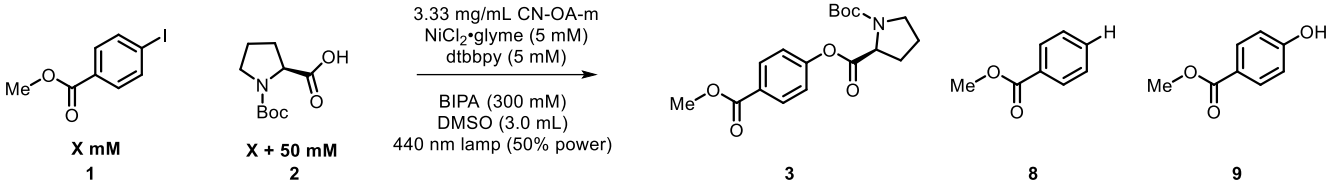

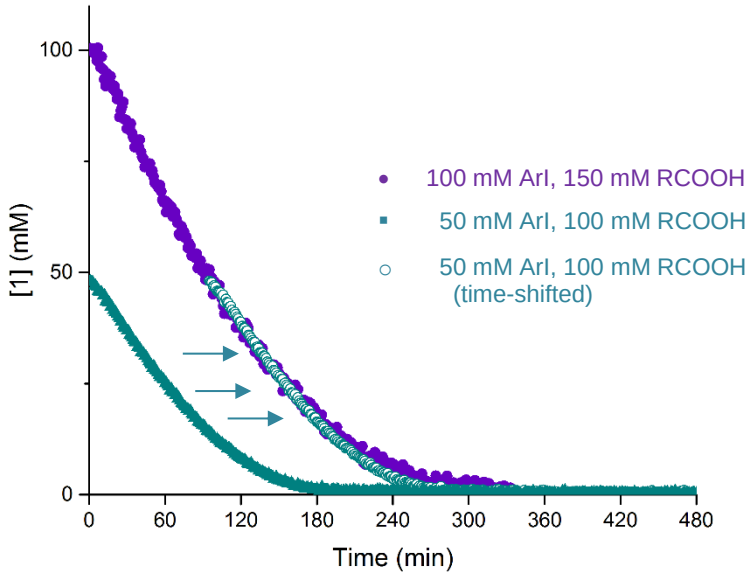

Figure S8. Overlay indicates no significant amount of catalyst deactivation or product inhibition in conditions outside of the linear absorption regime.

Entry	$[1]_0$	[1]	[3]	[8]	[9]	Total
jam209	100	0	96	3	2	101
jam214	50	0	45	2	2	49

Table S7. Tabulated yields and side products from photon-limited same excess experiment.

4.6 Different excess, aryl iodide

Following the delayed injection procedure (see section 2.1.3 – Ni•L delayed), experiments were conducted varying only the concentration of [**1**].

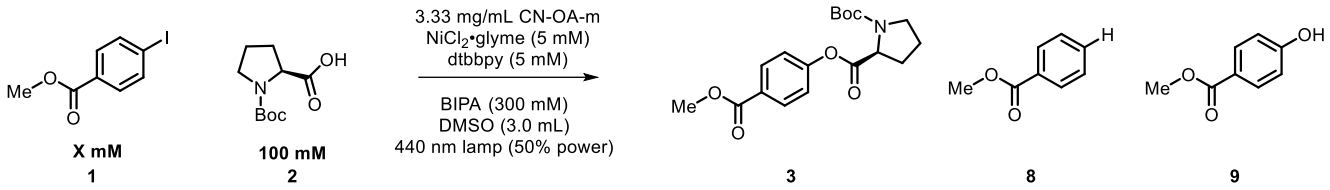

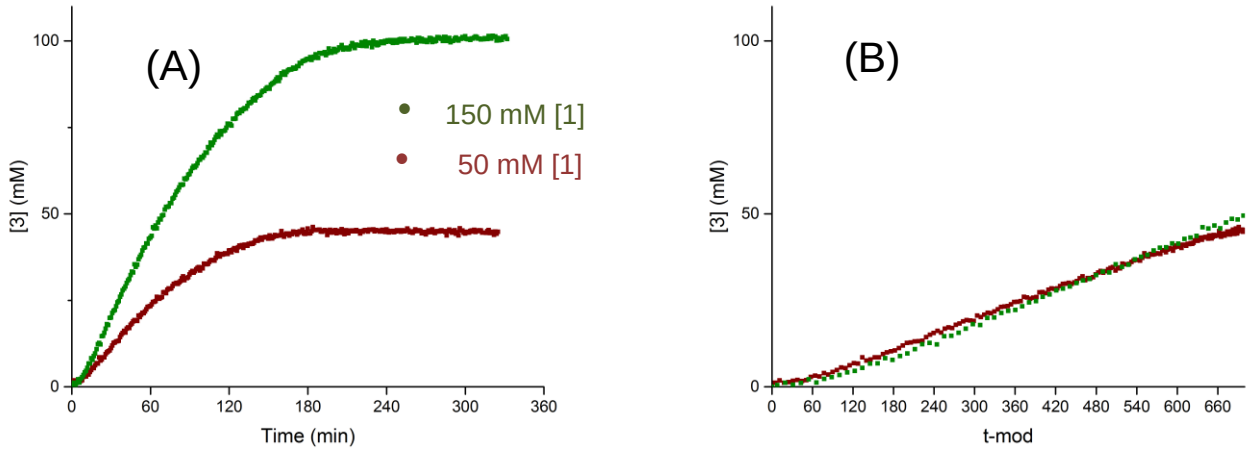

Figure S9. (A) Different excess experiments in the photon-limited regime show a positive-order dependence on [1]. (B) VTNA analysis shows best overlay at a coefficient of 0.5, indicating that rate ~[ArI]$^{0.5}$

Entry	$[1]_0$	[1]	[3]	[8]	[9]	Total
jam214	50	0	45	2	2	49
jam216	150	26	99	2	15	142

Table S8. Tabulated yields and side products from photon-limited different excess experiment.

4.7 Different excess, *N*-Boc proline

Following the delayed injection procedure (see section 2.1.3 – Ni•L delayed), experiments were conducted varying only the concentration of [2].

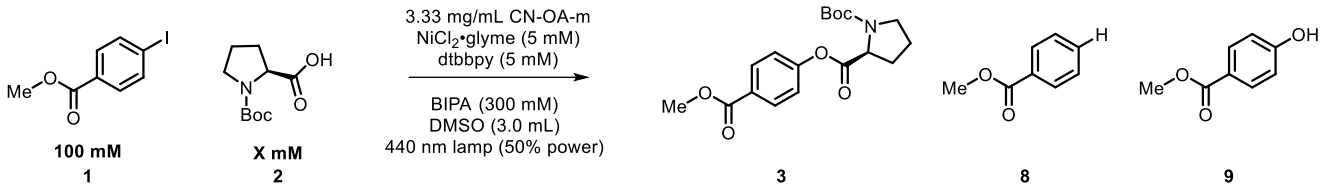

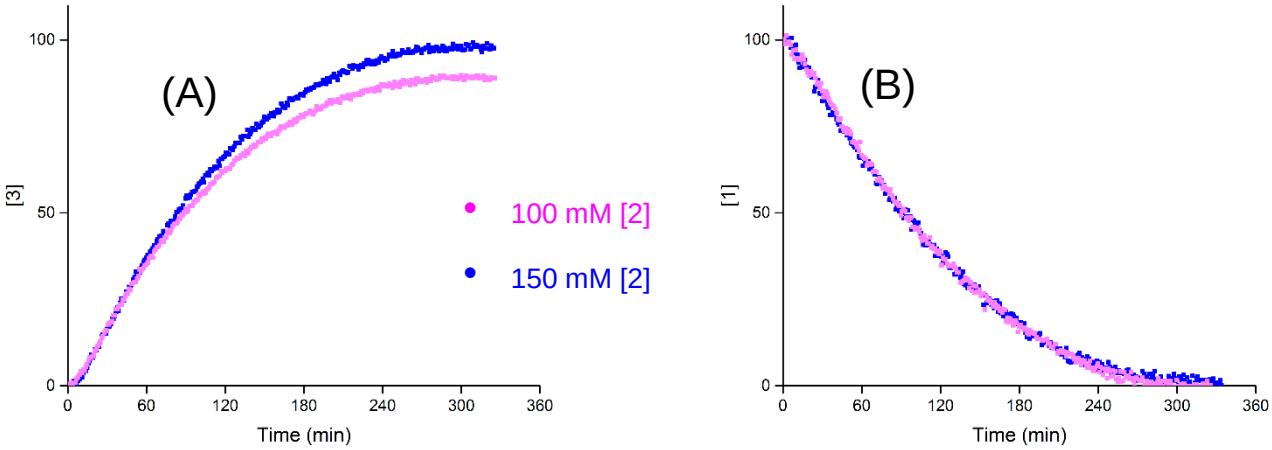

Figure S10. Different excess experiments in the photon-limited regime show a likely zero-order dependence on [2]. (A) Product formation. (B) Disappearance of substrate **1**.

Entry	$[2]_0$	[1]	[3]	[8]	[9]	Total
jam209	150	0	96	3	2	101
jam215	100	0	83	2	1	86

Table S9. Tabulated yields and side products from photon-limited different excess experiment.

5. Graphitic carbon nitride (heterogeneous) as photocatalyst: Photon-unlimited regime

5.1 Towards a photon-unlimited regime

Following the general procedure described above (see section 2.1.2), experiments were conducted varying only the concentration of nickel and ligand. Initial rates were determined with a Savitsky-Golay filter at the t = 15 min data point.

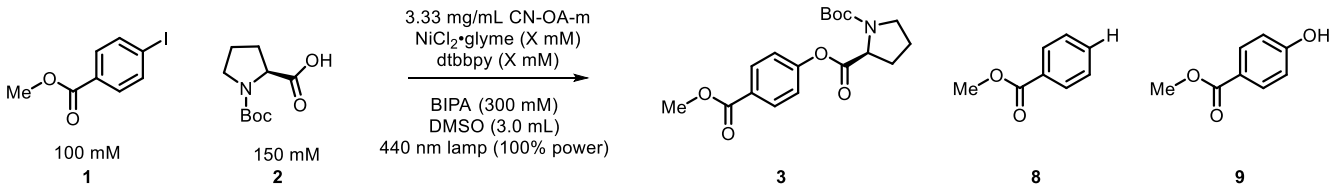

(Plot shown in Figure 2A.)

5.2 Catalyst order

Following the general procedure described above (see section 2.1.2), experiments were conducted varying only the concentration of nickel and ligand.

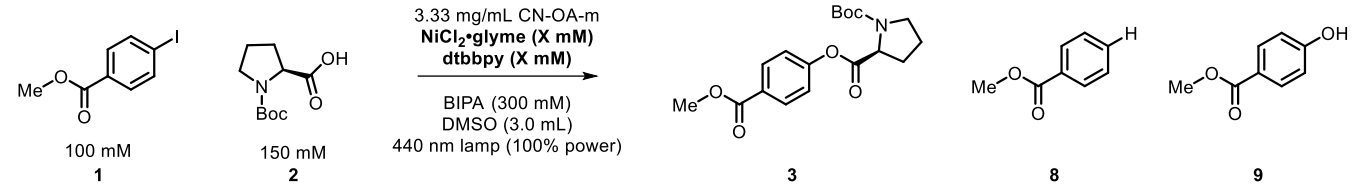

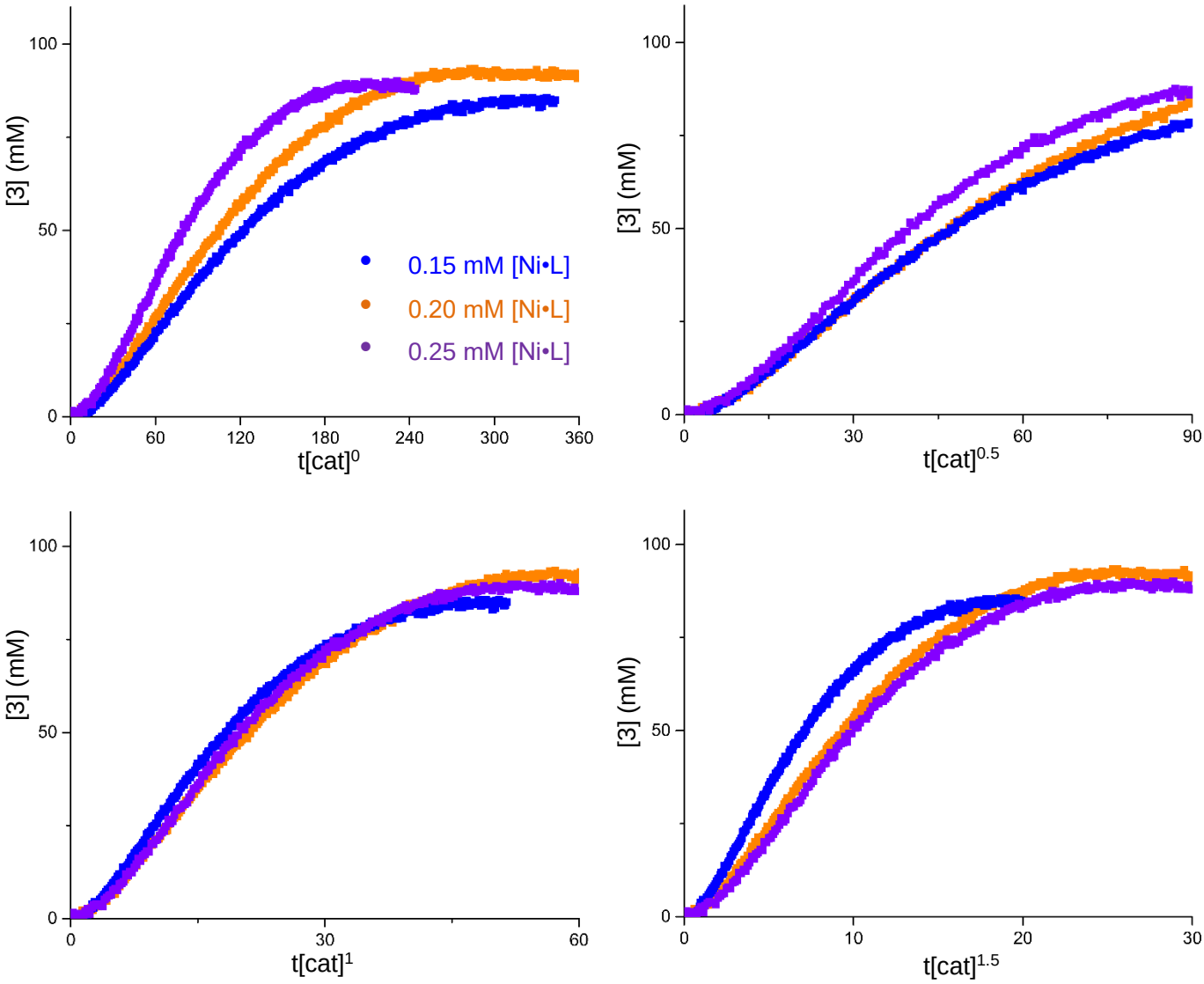

Figure S11. VTNA overlay indicates Ni•L is first order.

Entry	[Ni•L] (mM)	[1]	[3]	[8]	[9]	Total
jam281	0.15	0	85	5	5	95
jam278	0.20	0	88	5	6	99
jam284	0.25	0	87	4	5	96

Table S10. Tabulated yields and side products from photon-unlimited catalyst order experiments.

5.3 Same excess

Following the general procedure described above (see Section 2.1.2), experiments were conducted with the same excess (defined as [**2**]$_0$ – [**1**]$_0$; in this case 50 mM) but different initial concentrations.

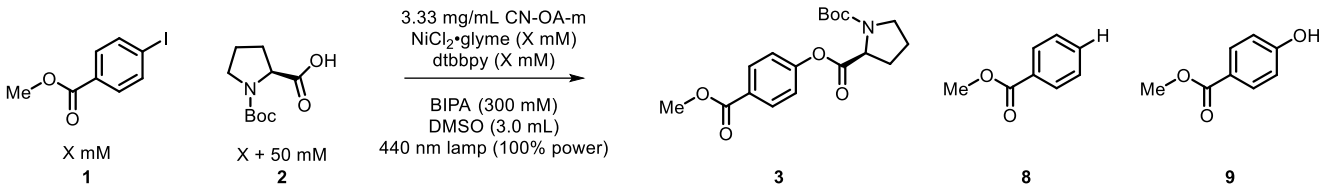

(Plot shown in Figure 2B.)

Entry	[1]$_0$	[1]	[3]	[8]	[9]	Total
jam278	100	0	88	5	6	99
jam287	50	0	41	4	4	49

Table S11. Tabulated yields and side products from photon-unlimited same excess experiments.

5.4 Different excess experiments, aryl iodide

5.4a General procedure

Following the general procedure described above (see Section 2.1.2), experiments were conducted varying only the concentration of [ArI].

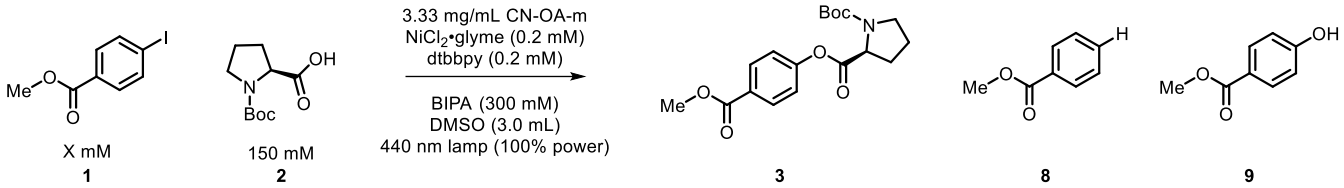

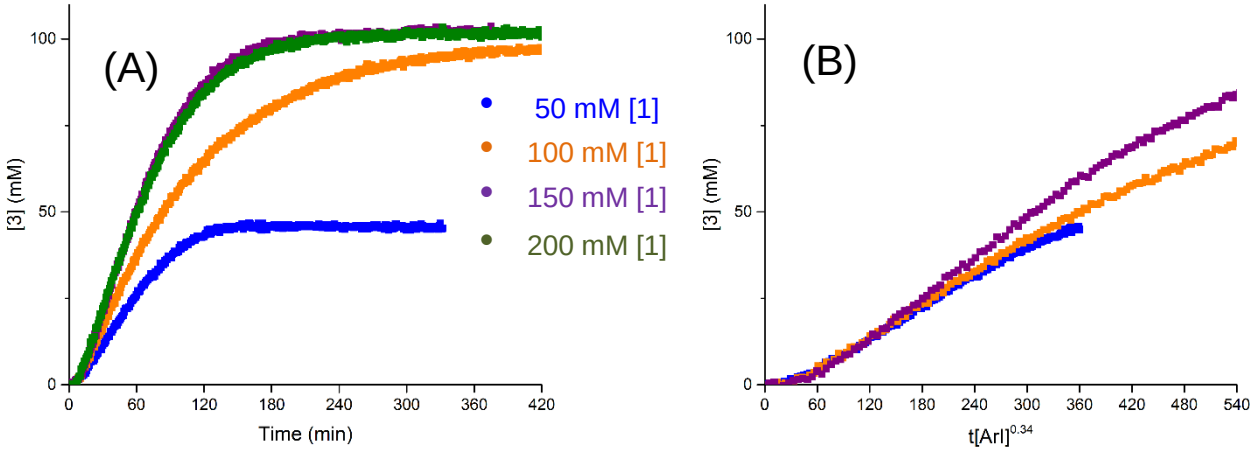

Figure S12. Attempted VTNA overlay was found to be difficult, likely due to the presence of an induction period. (A) Unprocessed [3] vs t data. (B) Best VTNA fit between coefficient 0.3 and 0.4.

Entry	$[1]_0$	[1]	[3]	[4]	[5]	Total
amCN6	50	0	45	3	3	51
amCN4	100	0	96	3	4	103
amCN5	150	25	102	6	14	147
amCN9	200	87	102	3	7	199

Table S12. Tabulated yields and side products from photon-unlimited aryl iodide order experiments.

5.4b Delayed injection procedure

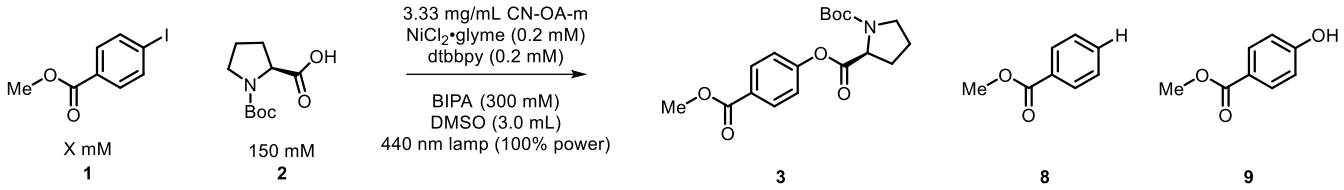

Following the delayed injection procedure (see section 2.1.3 – Ni•L delayed) described above, experiments were conducted varying only the concentration of [ArI]. Procedure B (delayed injection) was used.

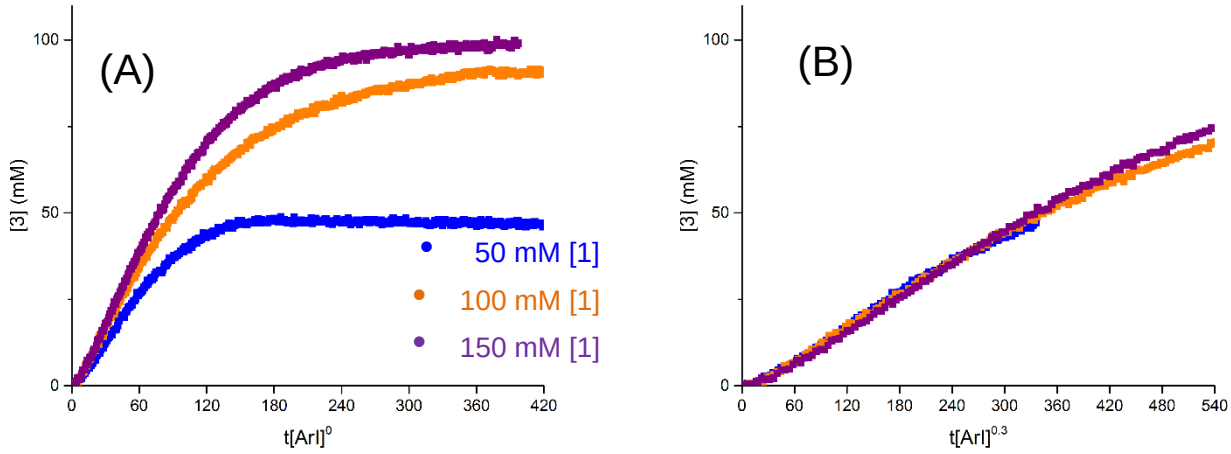

Figure S13. After delayed injection procedure, VTNA overlay found order of aryl iodide to be 0.3.

Entry	$[1]_0$	[1]	[3]	[8]	[9]	Total
amCN15	50	0	46	3	4	53
amCN12	100	0	91	3	5	99
amCN13	150	43	99	3	4	149

Table S13. Tabulated yields and side products from photon-unlimited aryl iodide order experiments, using a delayed injection to bypass the induction period and facilitate VTNA manipulation.

5.5 Different excess, *N*-Boc proline

Following the general procedure described above (see section 2.1.2), experiments were conducted varying only the concentration of carboxylic acid [**2**].

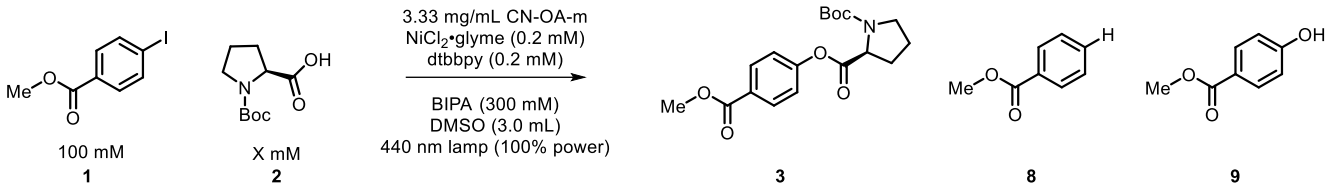

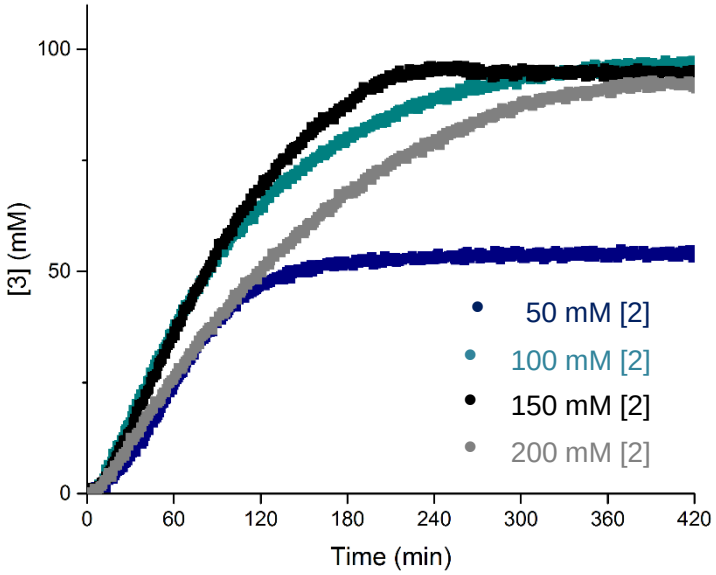

Figure S14. No VTNA manipulations were performed as the dependence on [2] is positive order until a threshold, after which point it becomes inhibitory.

Entry	$[2]_0$	[1]	[3]	[8]	[9]	Total
amCN20	50	17	52	20	8	97
amCN4	100	0	96	3	4	103
amCN3	150	0	93	4	4	101
amCN10	200	0	92	4	2	98

Table S14. Tabulated yields and side products from photon-unlimited experiments to determine rate dependence on [**2**].

5.6 Base experiments

Following the general procedure described above, experiments were conducted varying only the concentration of the secondary base *N-tert*-butylisopropylamine.

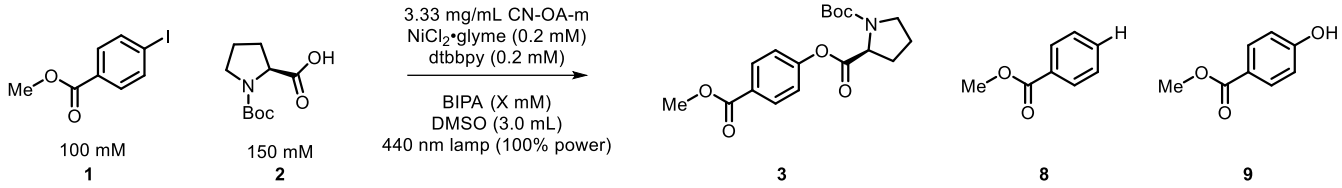

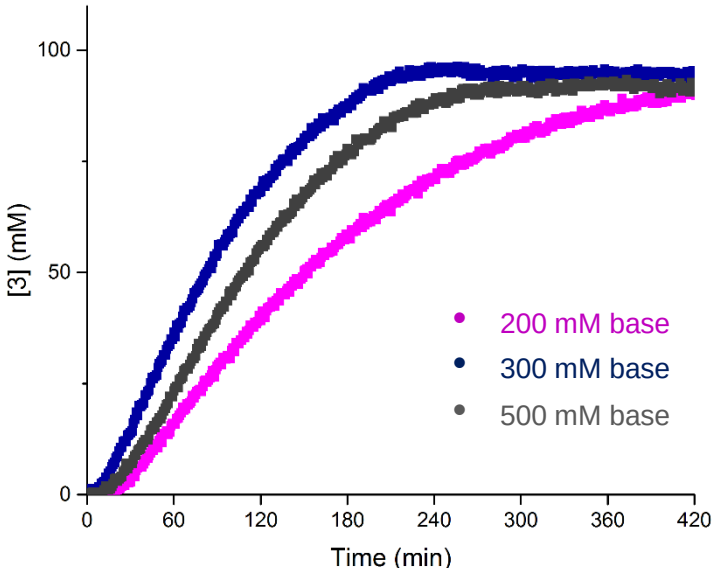

Figure S15. No VTNA manipulations were performed as the dependence on base is positive order until a threshold, after which point it becomes inhibitory.

Entry	[BIPA]	[1]	[3]	[8]	[9]	Total
amCN28	200	0	95	4	2	101
amCN3	300	0	93	4	4	101
amCN27	500	0	91	3	6	100

Table S15. Tabulated yields and side products from photon-unlimited experiments to determine rate dependence on base.

5.7 Photocatalyst experiments

Following the general procedure described above (see section 2.1.2), experiments were conducted varying only the loading of the photocatalyst.

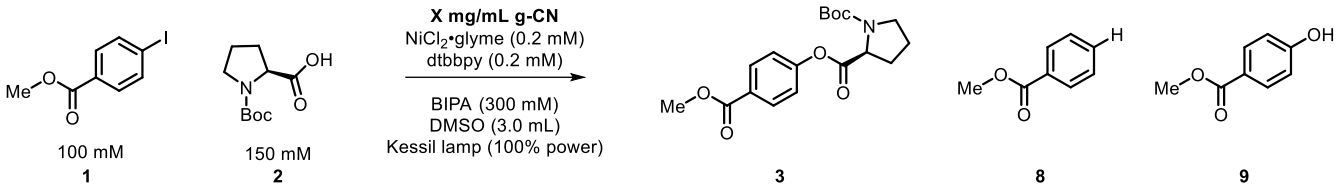

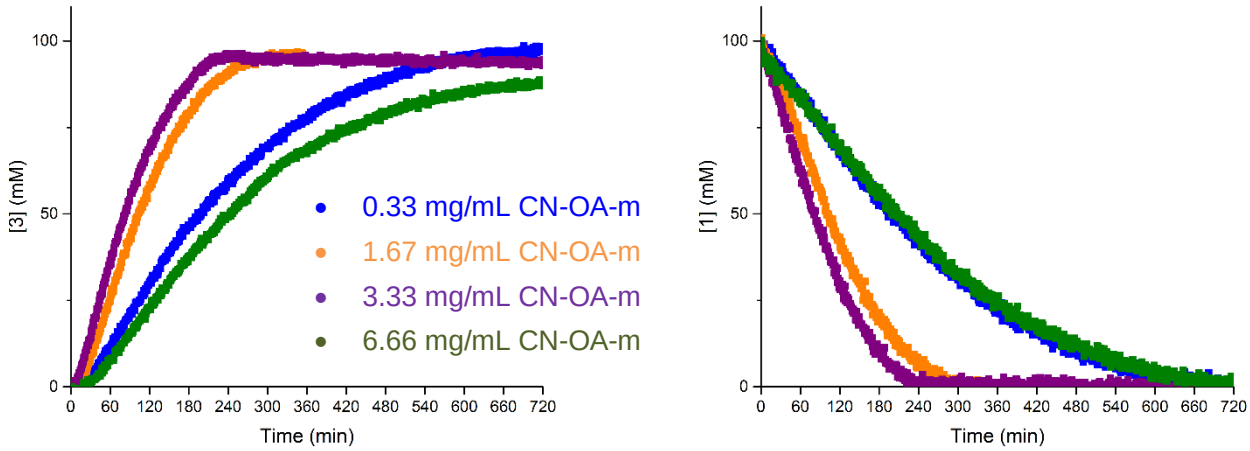

Figure S16. No VTNA manipulations were performed as the dependence on photocatalyst loading is positive order until a threshold, after which point it becomes inhibitory.

Entry	PC	[1]	[3]	[8]	[9]	Total
amCN39	0.33	0	97	2	0	99
amCN38	1.67	0	95	2	3	100
amCN3	3.33	0	93	4	4	101
amCN37	6.66	0	87	6	3	96

Table S16. Tabulated yields and side products from photon-unlimited experiments to determine rate dependence on heterogeneous photocatalyst loading.

5.8 Hammett plot

Following the general procedure described above (see section 2.1.2), experiments were conducted varying only the aryl iodide. Initial rates were determined with a Savitsky-Golay filter after the end of the induction period, which varied among halides in this series.

As in situ IR is an integral measurement,[3] obtaining rate data inherently produces lots of noise. As such, finding one 'initial rate' data point for extremely slow reactions is not possible with any reasonable amount of accuracy. For reactions that proceeded at a negligible pace, the initial rate was simply approximated as zero. For example, the most processed or smoothed (Savitsky-Golay filter, 19pt) rate data for the *p*-CH_3 substituent is shown below, from which any chosen value would have little significance.

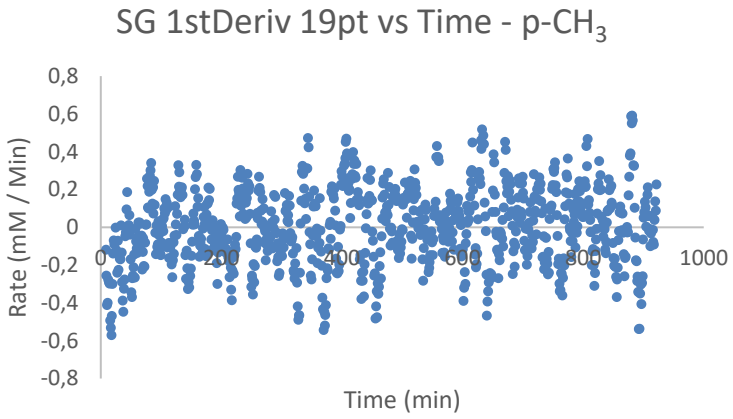

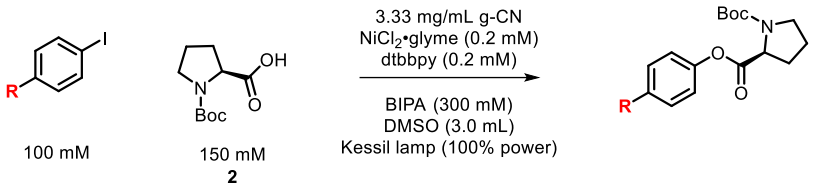

(Data shown graphically in Figure 4C.)

R	σ_{para}	Initial rate	log (k_R/k_H)
OCH3	-0.27	0	0
CH3	-0.17	0	0
H	0	0.06	0.00
Br	0.23	0.16	0.45
Cl	0.23	0.07	0.07
COCH3	0.5	0.76	1.12
CF3	0.54	0.81	1.15
CN	0.66	1.88	1.52

Table S17. Data used in Hammett study. Sigma para values obtained from literature.[4] Initial rates obtained from Savitsky-Golay filter applied to [**3**] vs t data. Concentrations of products obtained from NMR data that matches literature.[2]

6. $Ir(ppy)_3$ (homogeneous) as photocatalyst: Photon-limited regime

6.1 Determination of photocatalyst loading

Following the general procedure described above (see section 2.1.2), experiments were conducted varying only the concentration of photocatalyst.

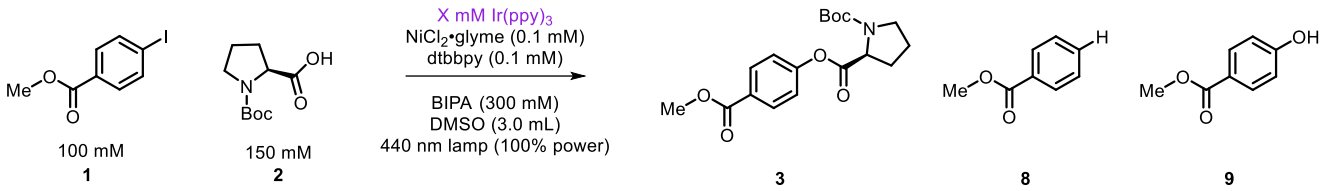

(Results of the reaction are presented in tabular form in Table 1 and graphical form in Figure 3A.)

When normalized [1] vs normalized [t] is plotted, the curvature change between the experiments becomes clearer:

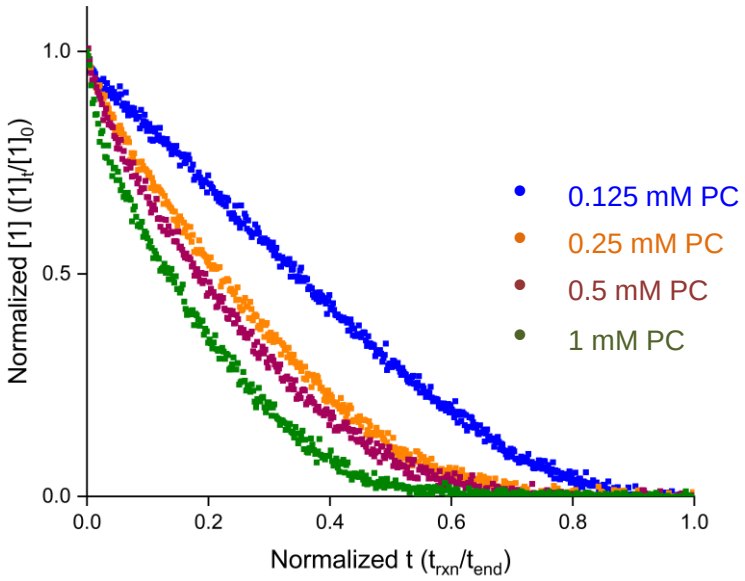

Figure S17. Flatter curvature of the lower photocatalytic loading is indicative of lower-order overall kinetics and a higher likelihood that rate is limited by photon-related processes.

6.1 Determination of nickel order

Following the general procedure described above (see section 2.1.2), experiments were conducted varying only the concentration of nickel and ligand.

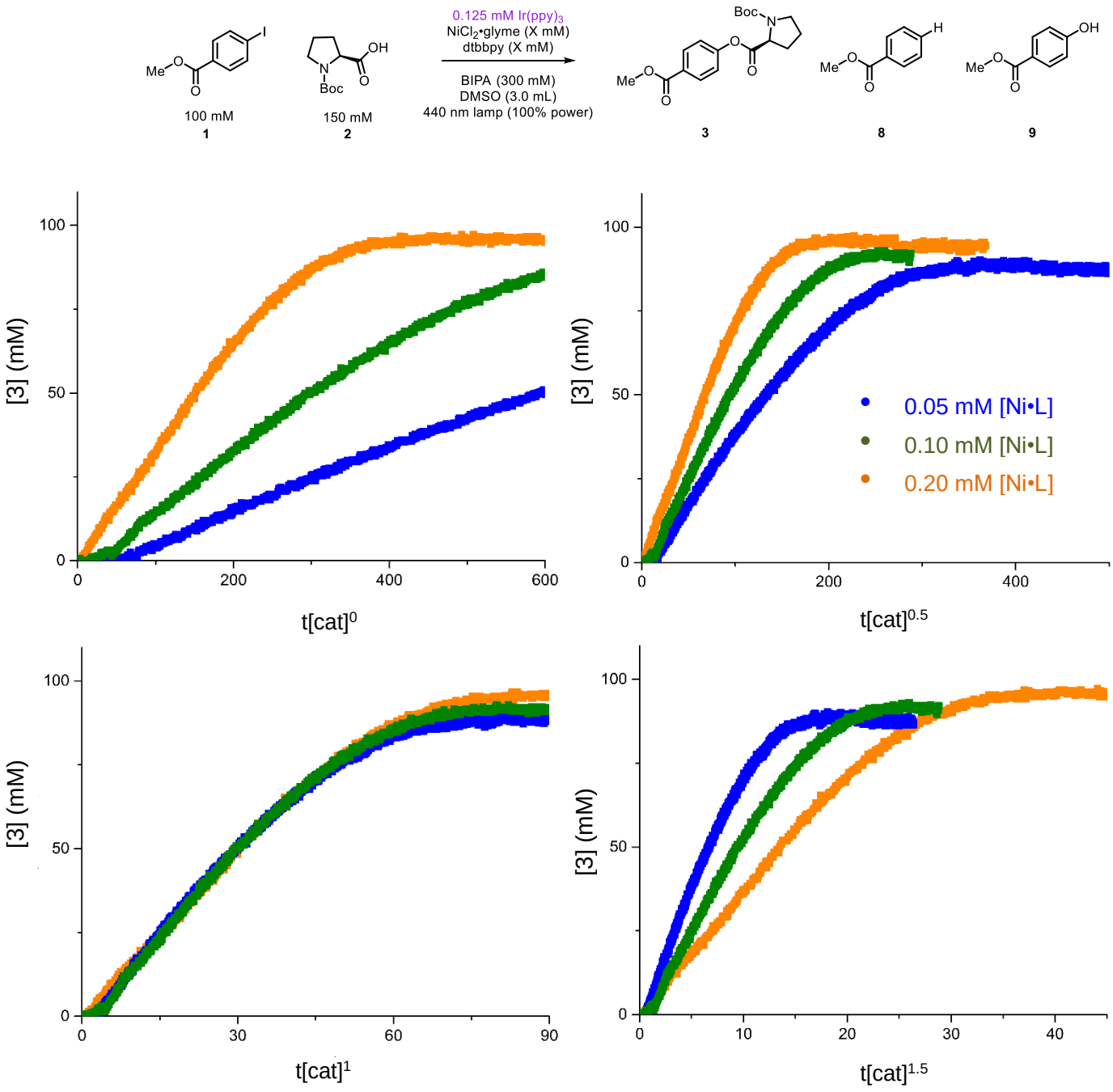

Figure S18. VTNA indicates that catalyst is first-order in the photon-limited regime of the homogeneous reaction.

Entry	[Ni•L]	[1]	[3]	[8]	[9]	Total
amIr21	0.05	0	87	5	3	95
amIr17	0.10	0	92	4	3	99
amIr16	0.20	0	94	3	4	101

Table S18. Tabulated yields and side products from photon-unlimited experiments assessing catalyst order.

6.2 Same excess

Following the general procedure outlined above (see section 2.1.2), two experiments were conducted with the same "excess" (50 mM) between $[1]_0$ and $[2]_0$.

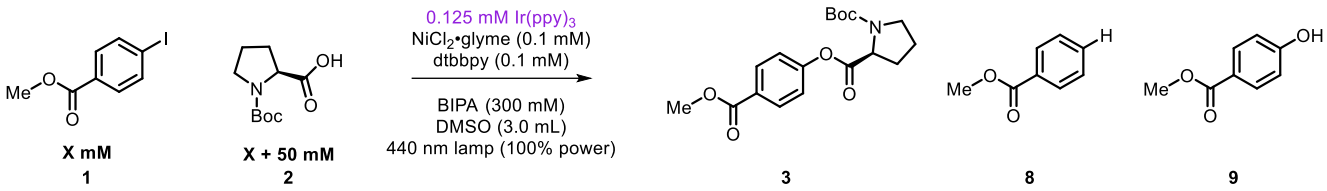

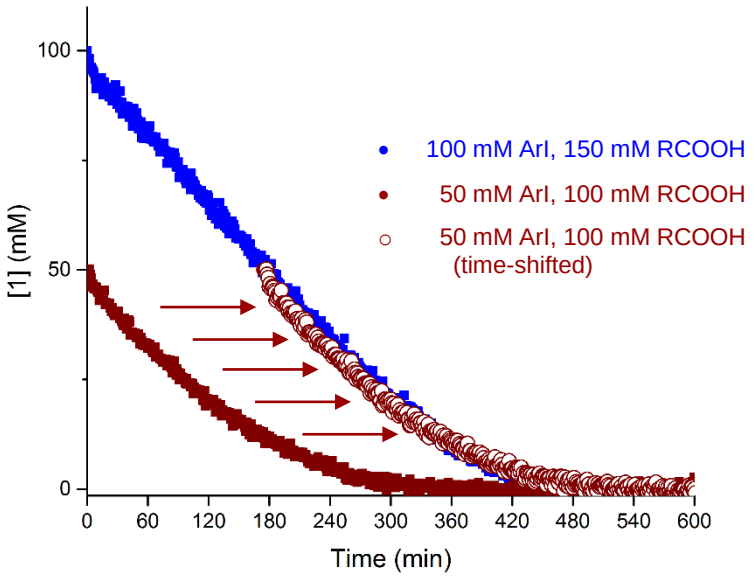

Figure S19. Same excess experiment for the photon-limited homogeneous reaction, in contrast to the photon-unlimited regime, shows no significant amounts of catalyst deactivation.

Entry	$[1]_0$	[1]	[3]	[8]	[9]	Total
amIr29	100	0	86	5	5	96
amIr28	50	1	41	3	3	48

Table S19. Tabulated yields and side products from homogeneous photon-limited same excess experiment.

6.3 Different excess experiments

Following the general procedure described above (see section 2.1.2), experiments were conducted varying only the concentrations of aryl iodide **1** and carboxylic acid **2**.

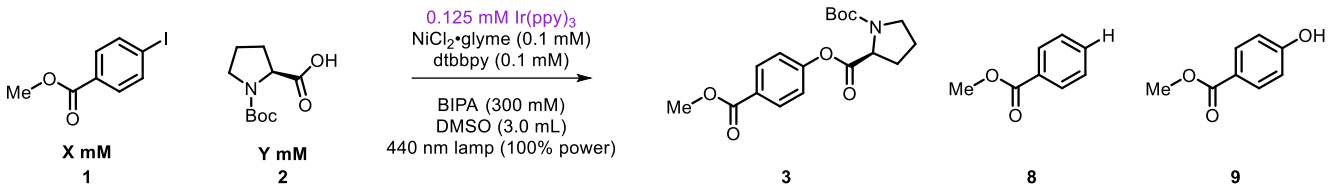

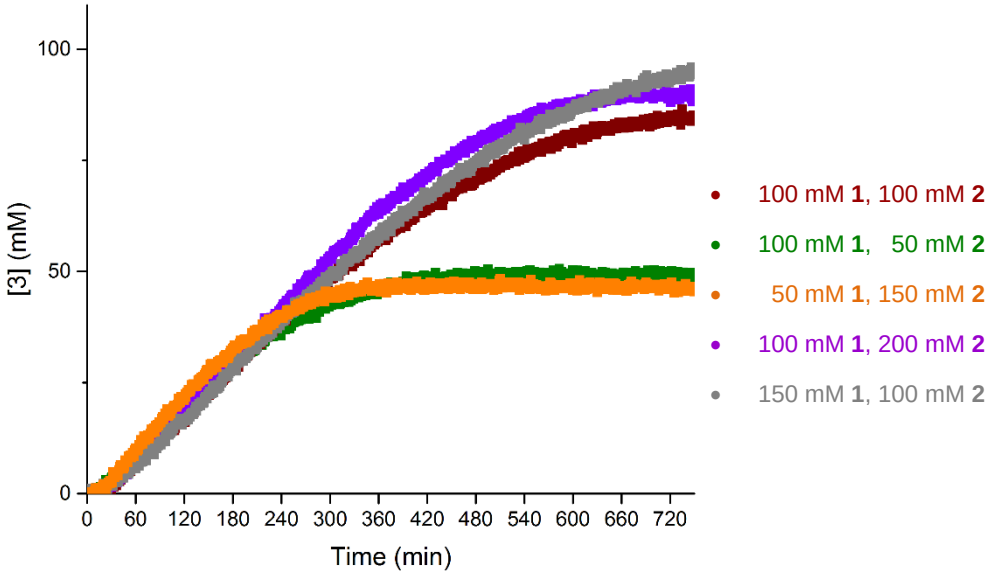

Figure S20. Different excess experiments varying the starting concentrations of **1** and **2** show dependence on neither.

Entry	$[1]_0$	$[2]_0$	[1]	[3]	[8]	[9]	Total
amIr31	100	100	1	88	4	7	100
amIr33	100	50	22	50	6	19	97
amIr41	50	150	0	47	3	1	51
amIr42	100	200	0	93	5	3	101
amIr43	150	100	26	100	6	16	148

Table S20. Tabulated yields and side products from homogeneous photon-limited different excess experiments.

6.4 Base experiments

Following the general procedure described above (see section 2.1.2), experiments were conducted varying only the concentrations of base.

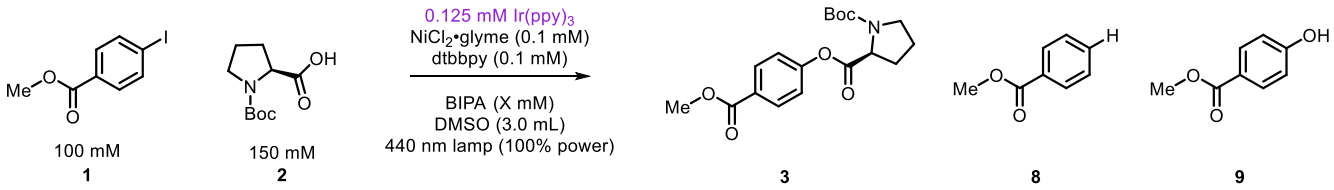

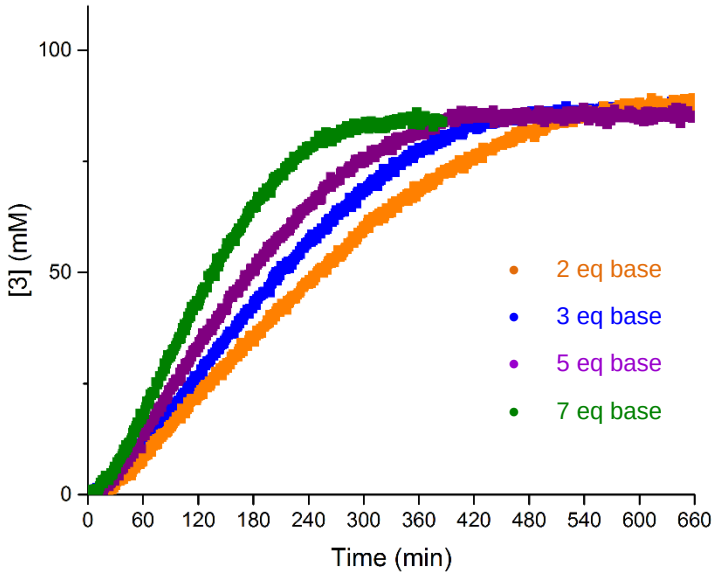

Figure S21. Varying concentration of base was the only factor that could accelerate the homogeneous reaction in the photon-limited regime.

Entry	[BIPA]	[1]	[3]	[8]	[9]	Total
amIr49	200	0	89	5	1	95
amIr29	300	0	86	5	5	96
amIr48	500	0	83	7	4	94
amIr50	700	0	84	7	6	97

Table S21. Tabulated yields and side products from base studies of the homogeneous photon-limited regime.

7. $Ir(ppy)_3$ (homogeneous) as photocatalyst: Photon-unlimited regime, 0.2 mM [Ni•L]

7.1 Determination of photocatalyst loading

Following the general procedure described above (see section 2.1.2), experiments were conducted varying only the concentration of photocatalyst.

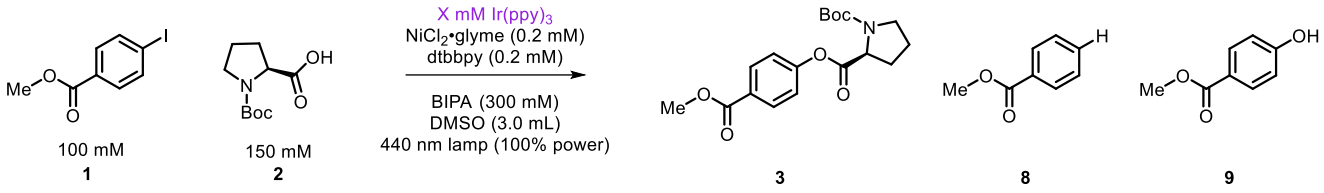

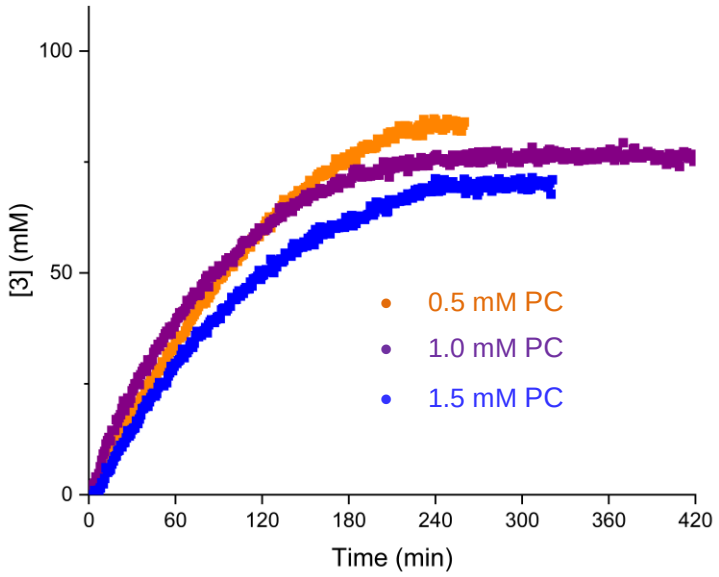

Figure S22. Varying concentration of PC to find regime in which nickel catalyst would be saturated with excited photocatalyst species.

Entry	[PC]	[1]	[3]	[8]	[9]	Total
jam325	0.5	0	84	6	2	92
jam326	1.0	0	73	11	3	87
jam327	1.5	0	71	11	2	84

Table S22. Tabulated yields and side products from PC studies of the homogeneous O-arylation.

7.1.1 Towards a photon-unlimited regime – VTNA test, 0.5 mM PC

It appeared that both 0.5 mM and 1.0 mM PC were candidates for a photon-unlimited regime with 0.2 mM Ni•L. The lowest possible PC loading would be preferable as higher PC loadings gave more side product. To test if we were in a photon-unlimited regime, we performed VTNA on experiments varying nickel concentrations, similar to sections 4.3, 5.2, and 6.2; if nickel is first-order, we are in such a regime.

Following the general procedure described above (see section 2.1.2), experiments were conducted varying only the concentration of nickel and ligand.

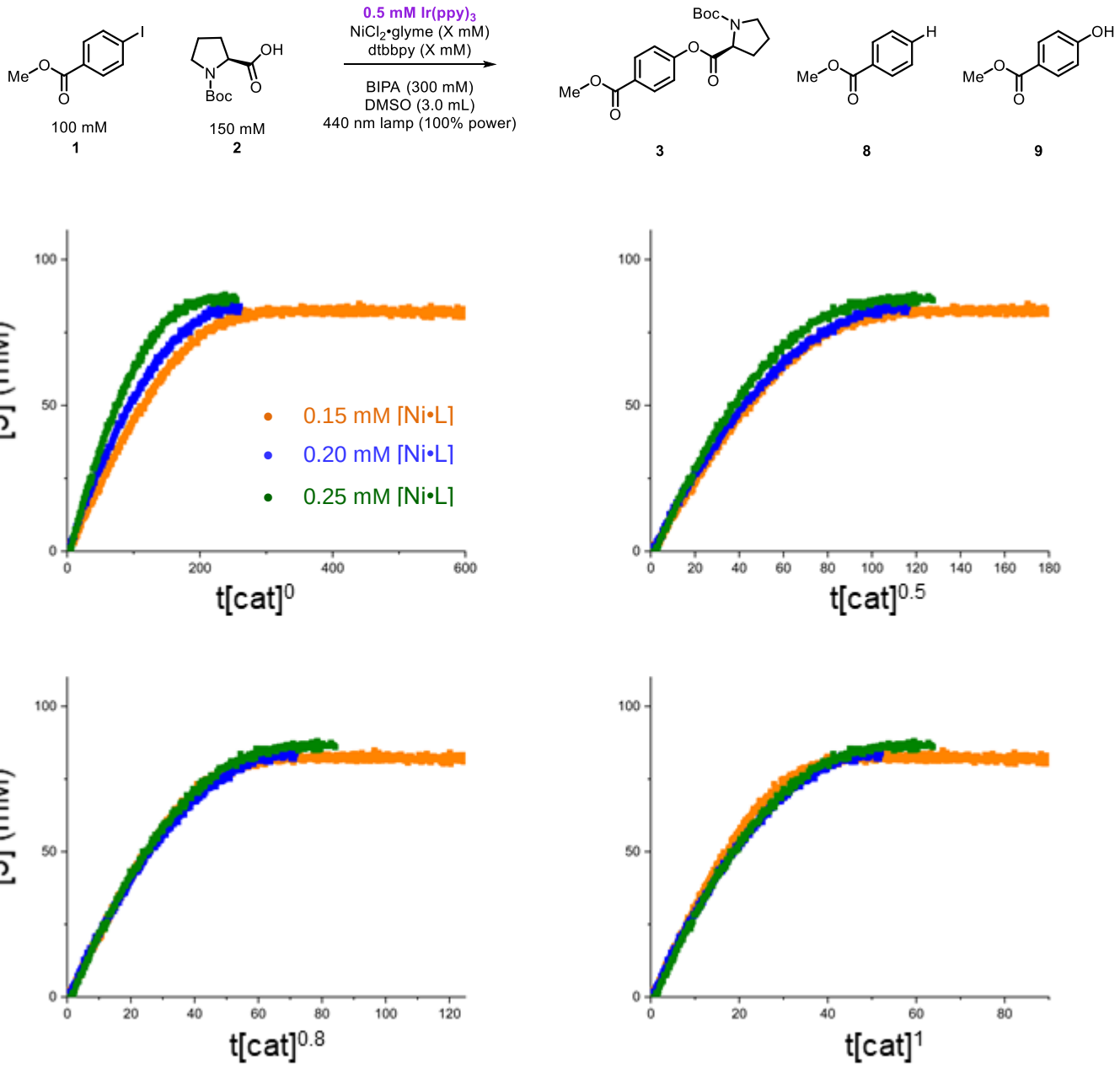

Figure S23. At 0.5 mM PC, nickel could be considered first-order around 0.20 mM, but high fractional was the most accurate overlay.

Entry	[Ni•L]	[1]	[3]	[8]	[9]	Total
jam328	0.15	0	80	8	4	92
jam325	0.20	0	84	6	2	92
jam329	0.25	0	86	5	2	93

Table S23. Tabulated yields and side products from experiments assessing catalyst order at 0.5 mM $Ir(ppy)_3$.

7.1.2 Towards a photon-unlimited regime – VTNA test, 1.0 mM PC

While a photocatalyst loading of 0.5 mM $Ir(ppy)_3$ showed high fractional order for Ni•L around 0.2 mM, it was theorized that increasing the PC loading would ensure first-order kinetics.

Following the general procedure described above (see section 2.1.2), experiments were conducted varying only the concentration of nickel and ligand.

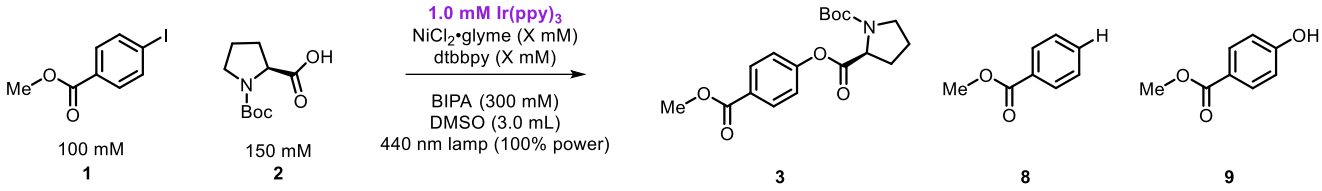

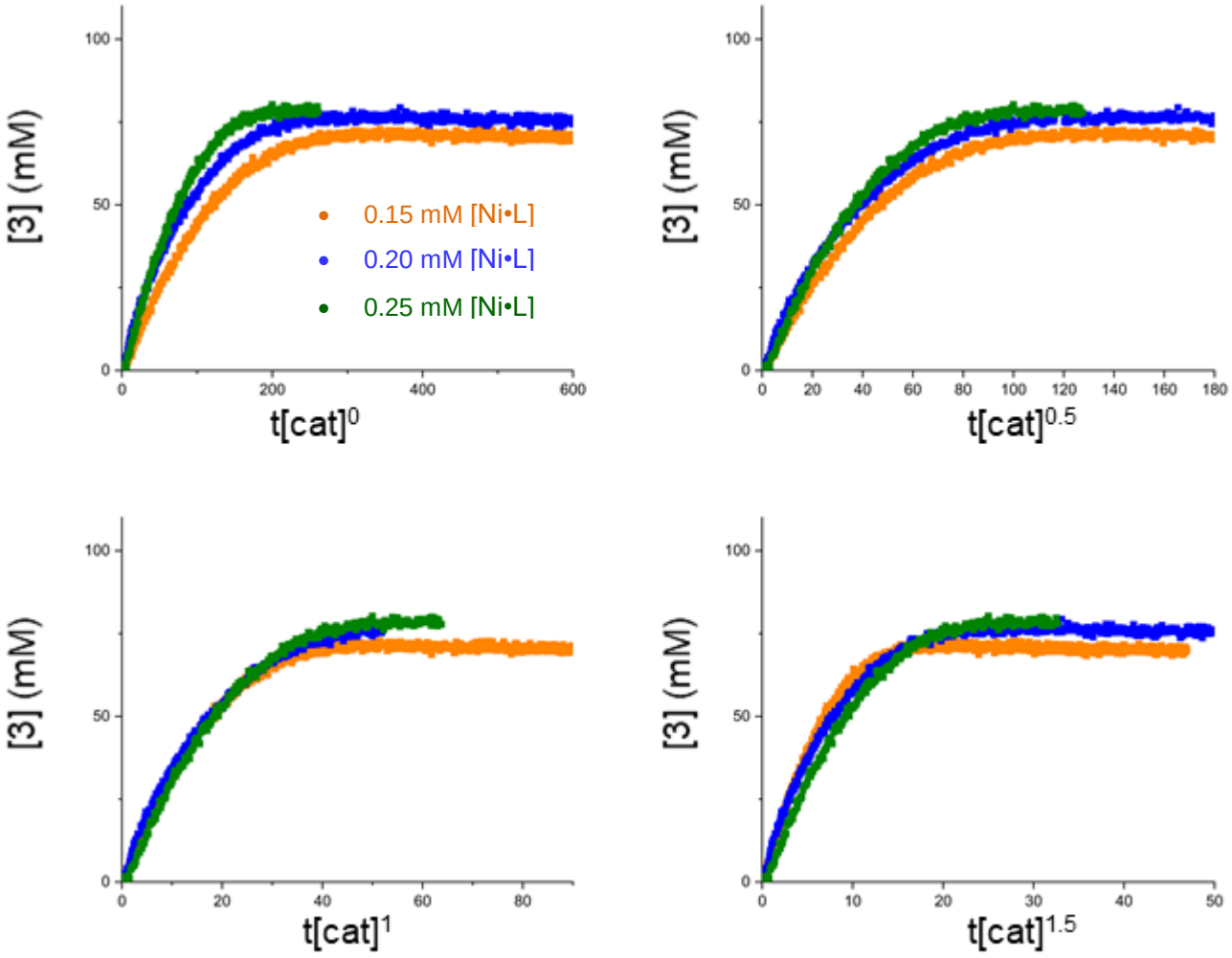

Figure S24. VTNA indicates that nickel catalyst is first-order at 1.0 mM $Ir(ppy)_3$.

Entry	[Ni•L]	[1]	[3]	[8]	[9]	Total
jam330	0.15	0	70	11	3	84
jam326	0.20	0	73	11	3	87
jam331	0.25	0	78	9	3	90

Table S24. Tabulated yields and side products from experiments assessing catalyst order at 1.0 mM $Ir(ppy)_3$.

7.2 Same excess

Following the general procedure outlined above (see section 2.1.2), two experiments were conducted with the same “excess” (50 mM) between $[1]_0$ and $[2]_0$.

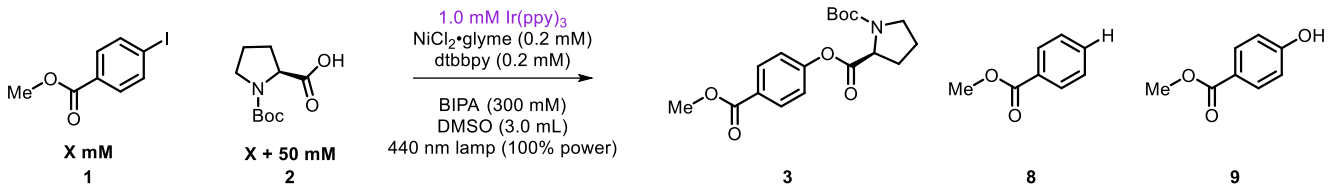

(Plot shown in Figure 3B.)

Entry	$[1]_0$	[1]	[3]	[8]	[9]	Total
jam326	100	0	73	11	3	87
jam332	50	0	35	5	2	42

Table S25. Tabulated yields and side products from homogeneous photon-unlimited same excess experiment.

7.3 Different excess experiments, aryl iodide

Following the general procedure outlined above (see section 2.1.2), experiments were conducted varying only the concentration of aryl iodide **1**.

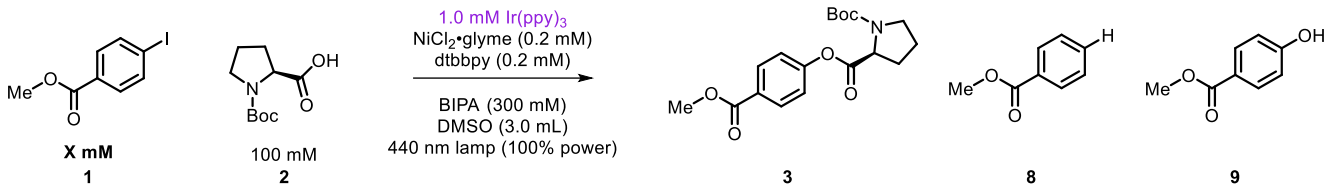

(Plot shown in Figure 3C.)

Entry	$[1]_0$	[1]	[3]	[8]	[9]	Total
jam334	150	6	92	16	14	128
jam333	100	0	72	11	5	88
jam335	50	0	35	5	2	42
jam338	25	0	16	2	4	22
jam339	10	0	6	1	1	8

Table S26. Tabulated yields and side products from homogeneous photon-unlimited different excess experiments varying $[1]_0$.

7.4 Different excess experiments, N-Boc proline

Following the general procedure outlined above (see section 2.1.2), experiments were conducted varying only the concentration of *N*-Boc proline **2**.

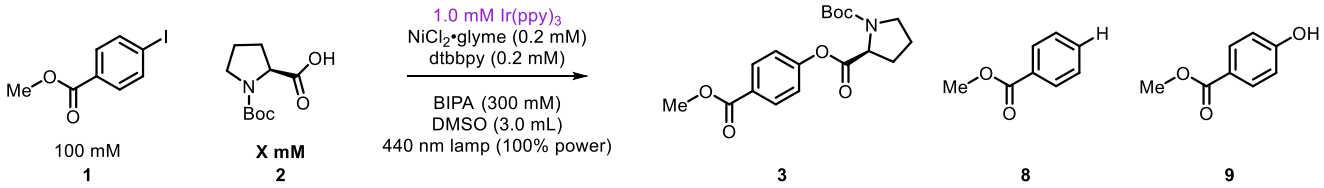

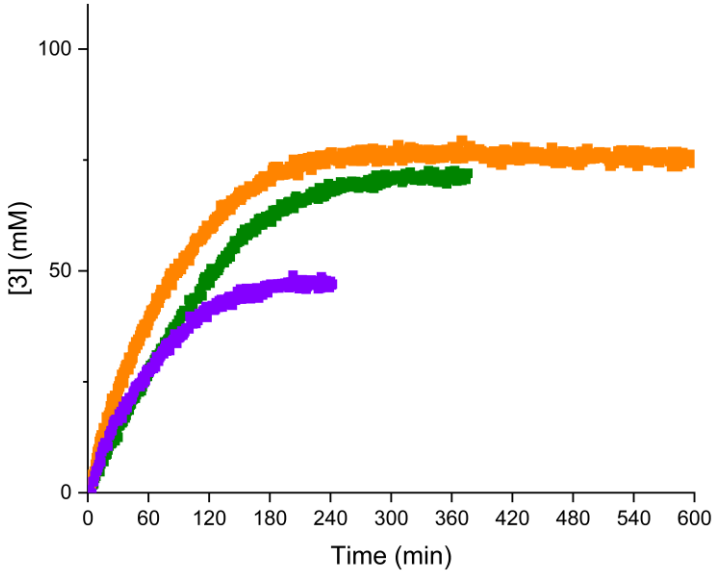

Figure S25. The dependence on [2] is not solvable through VTNA analysis.

Entry	$[2]_0$	[1]	[3]	[8]	[9]	Total
jam326	150	0	73	11	3	87
jam333	100	0	72	11	5	88
jam337	50	10	47	13	14	84

Table S27. Tabulated yields and side products from homogeneous photon-unlimited different excess experiments varying $[2]_0$.

7.5 Base experiments

Following the general procedure outlined above (see section 2.1.2), experiments were conducted varying only the concentration of base.

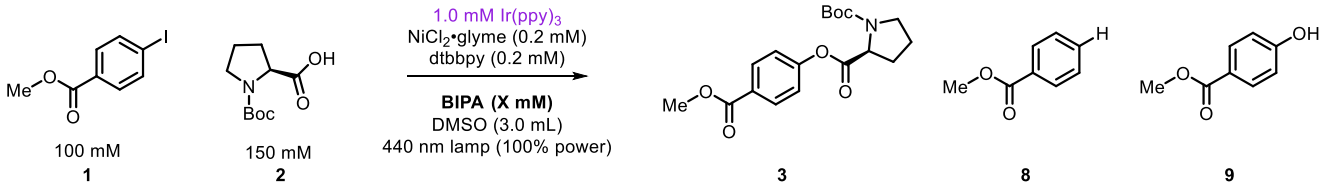

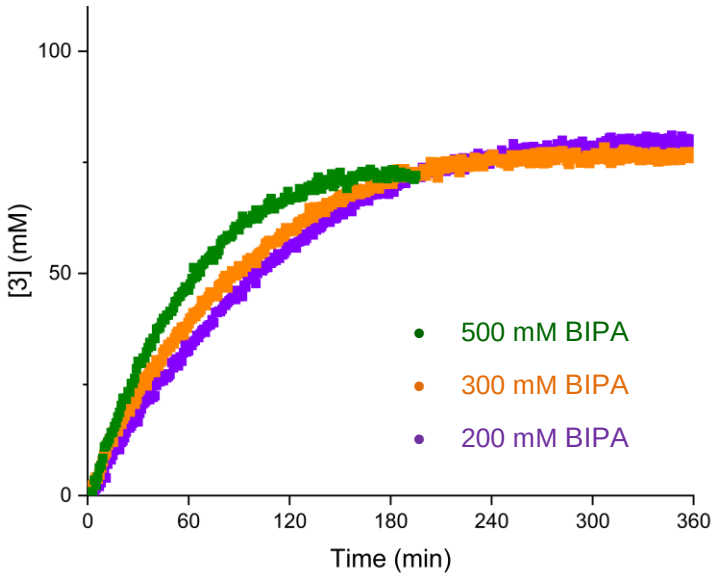

Figure S26. Increasing concentration of base accelerates the homogeneous reaction in the photon-unlimited regime.

Entry	[BIPA]	[1]	[3]	[8]	[9]	Total
jam336	200	0	80	9	3	92
jam326	300	0	73	11	3	87
jam335	500	0	72	12	6	90

Table S28. Tabulated yields and side products from homogeneous photon-unlimited different excess experiments varying [base].

8. $Ir(ppy)_3$ (homogeneous) as photocatalyst: Photon-unlimited regime, classically derived [Ni•L]

The purpose of this section was to corroborate the data from Section 7 through finding the linear-absorption (photon-unlimited) regime through the same procedure that was used in the *heterogeneous* case. These data sets are the same as Section 7 but with a lower [PC] and [Ni]. Agreement between Sections 7 and 8 helps reinforce that the regime is photon-unlimited. The reaction times are longer in this section, but otherwise the trends are the same as Section 7. This remains as a note for researchers that the photon-unlimited regime can be accessed through either procedure.

8.1 Toward a photon-unlimited regime: Initial rate studies, 0.5 mM $Ir(ppy)_3$

Following the general procedure described above (see section 2.1.2), experiments were conducted varying only the concentration of nickel and ligand. Initial rates were determined from product formation with a Savitsky-Golay filter at the t = 10 min data point.

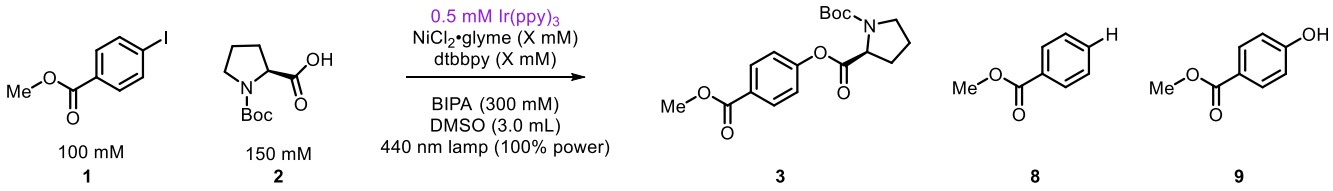

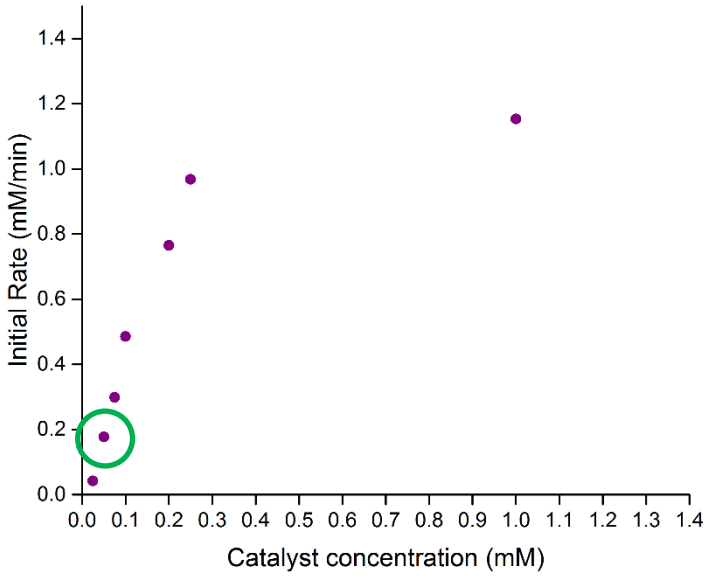

Figure S27. Initial rate studies performed to determine region in which nickel catalyst is not limited by transfer from excited photocatalytic species.

8.2 Order of nickel catalyst, photon-unlimited

Following the general procedure described above (see section 2.1.2), experiments were conducted varying only the concentration of nickel and ligand.

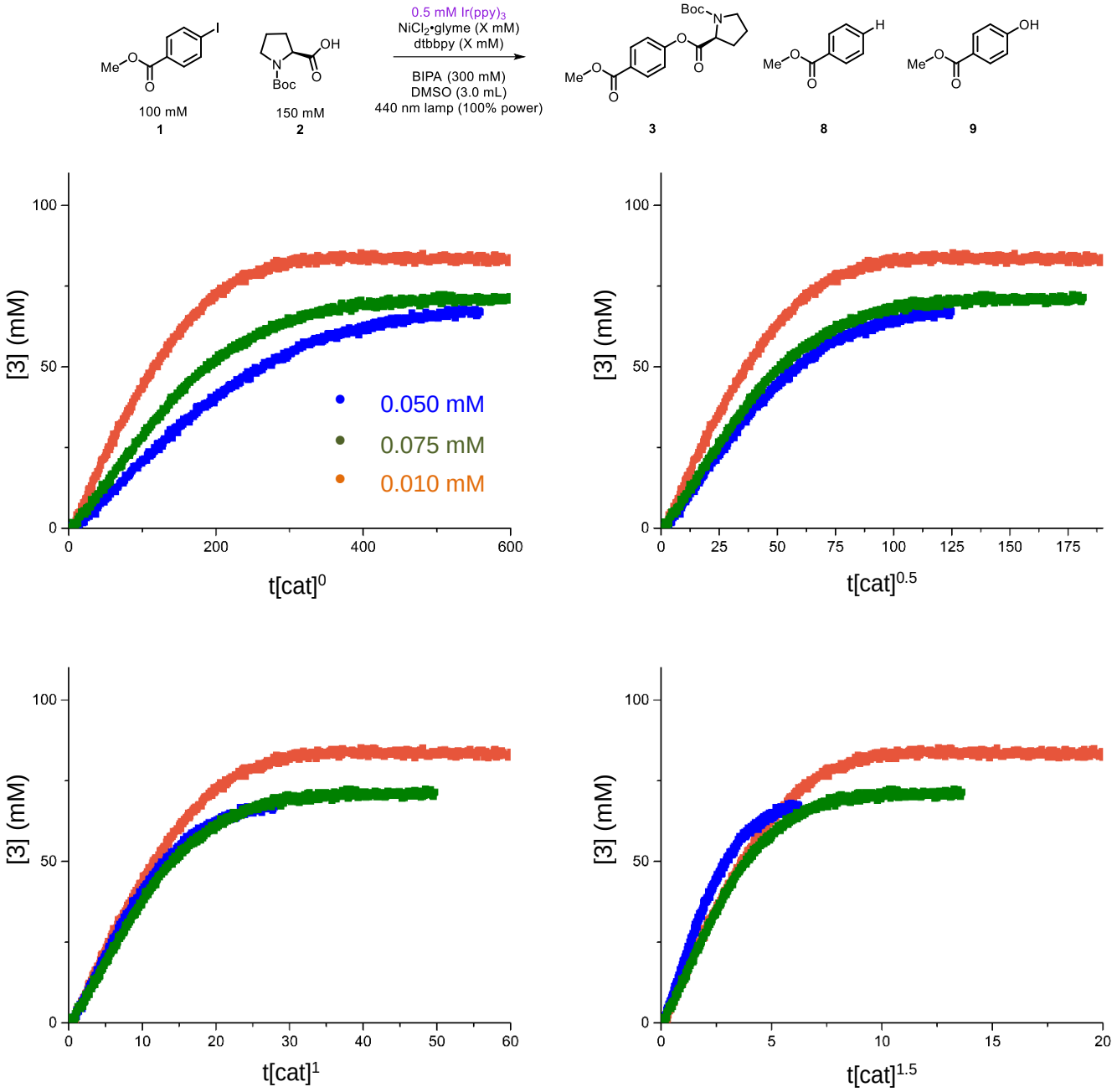

Figure S28. VTNA indicates that catalyst is first-order.

Entry	[Ni]	[1]	[3]	[8]	[9]	Total
amIr63	0.050	1	67	12	2	82
amIr61	0.075	0	73	11	3	87
amIr51	0.100	0	82	8	3	93

Table S29. Tabulated yields and side products from photon-unlimited catalyst order experiments.

8.3 Same excess

Following the general procedure described above (see Section 2.1.2), experiments were conducted with the same excess (defined as [**2**]$_0$ – [**1**]$_0$; in this case 50 mM) but different initial concentrations.

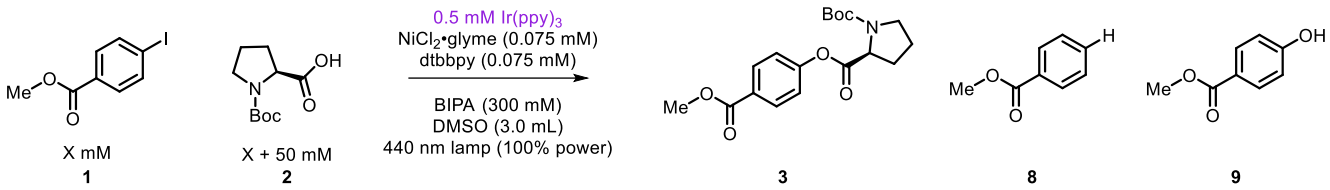

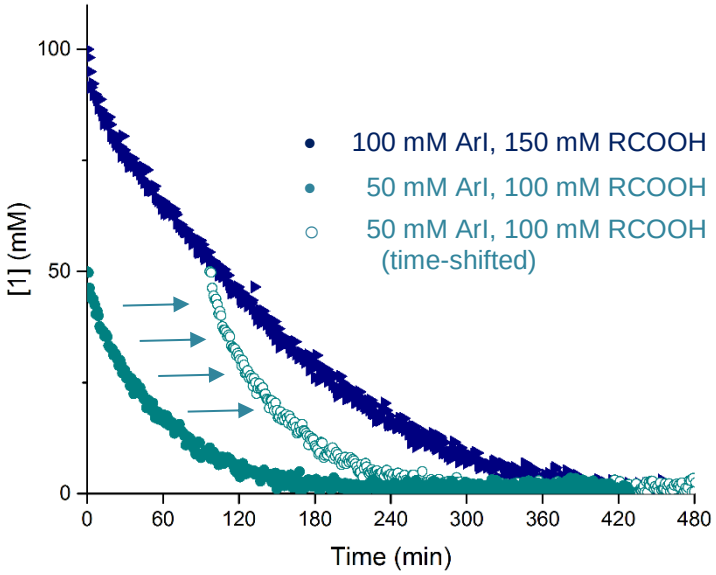

Figure S29. Same excess experiment indicates catalyst deactivation occurs in the photon-unlimited regime for the homogeneous reaction.

Entry	[1]$_0$	[1]	[3]	[8]	[9]	Total
amIr64	50	0	35	7	2	44
amIr61	100	0	73	11	3	87

Table S30. Tabulated yields and side products from photon-unlimited same excess experiments.

8.4 Different excess

Following the general procedure described above (see section 2.1.2), experiments were conducted varying only the concentrations of aryl iodide **1** and carboxylic acid **2**.

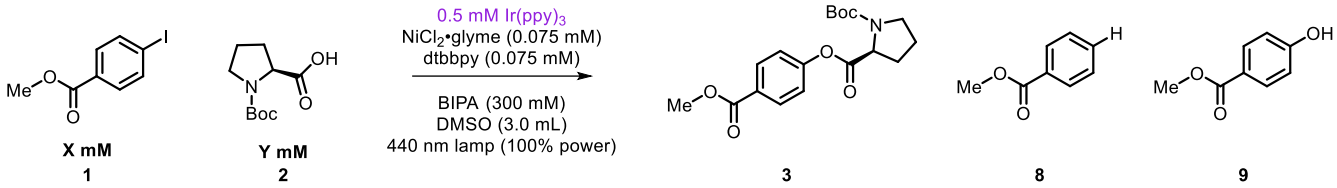

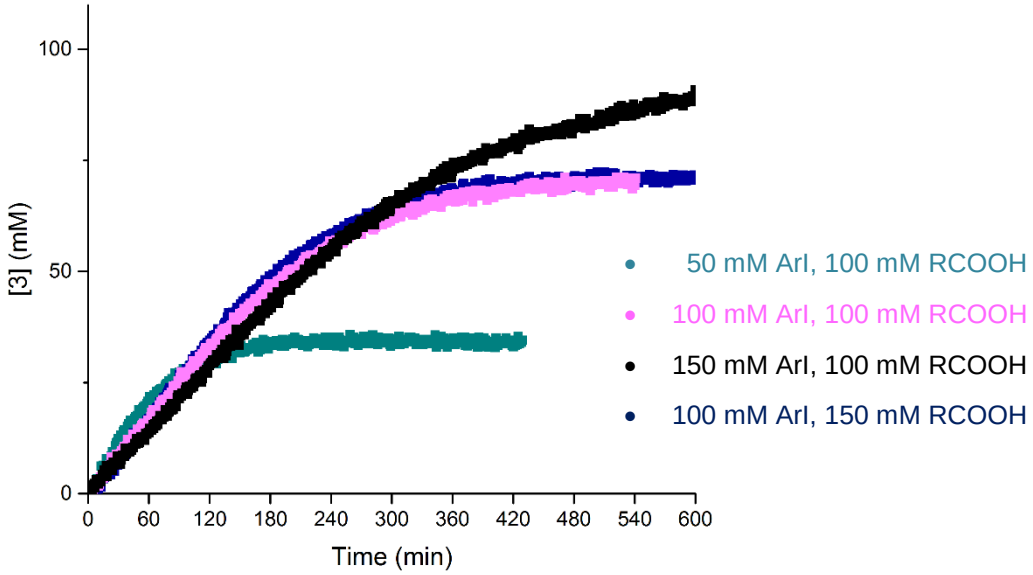

Figure S30. Different excess experiments indicate a lack of rate dependence on [1] or [2] for photon-unlimited homogeneous reactions.

Entry	$[1]_0$	$[2]_0$	[1]	[3]	[4]	[5]	Total
amIr64	50	100	0	35	7	2	44
amIr65	100	100	0	71	12	4	87
amIr66	150	100	17	92	17	8	134
amIr61	100	150	0	73	11	3	87

Table S31. Tabulated yields and side products from photon-unlimited experiments assessing reagent orders of substrates.

8.5 Base experiments

Following the general procedure described above, experiments were conducted varying only the concentration of base.

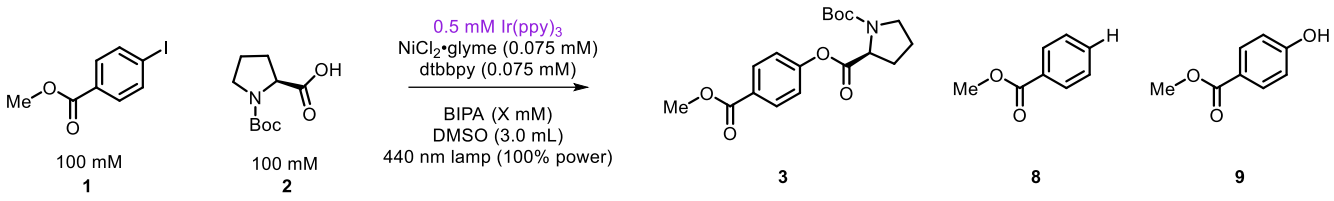

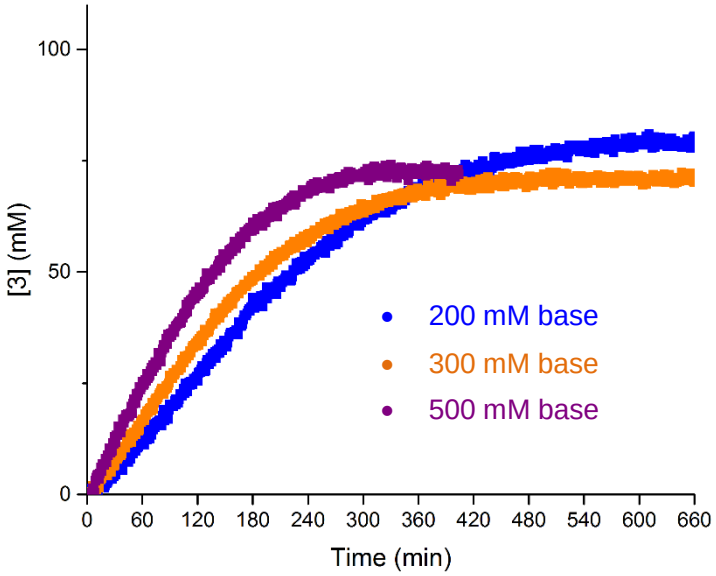

Figure S31. Experiments varying the amount of base in the photon-unlimited, homogeneous reaction.

Entry	[BIPA] (mM)	[1]	[3]	[8]	[9]	Total
amIr68	200	0	80	10	2	92
amIr61	300	0	73	11	3	87
amIr69	500	0	72	14	5	91

Table S32. Tabulated yields and side products from photon-unlimited experiments assessing role of base.

[1] *J. Org. Chem.* **1999**, *64*, 6263
[2] *Angew. Chem. Int. Ed.* **2019**, *58*, 9575
[3] *Angew. Chem. Int. Ed*. **2005**, *44*, 4302
[4] *Chem. Rev.* **1991**, *91*, 165.